



HHS Public Access

Author manuscript

Nature. Author manuscript; available in PMC 2021 January 08.

Published in final edited form as:

Nature. 2020 August ; 584(7821): 415–419. doi:10.1038/s41586-020-2462-y.

Fitness trade-offs incurred by ovary-to-gut steroid signaling in *Drosophila*

Sara Mahmoud H. Ahmed^{1,2,3}, Julieta A. Maldera¹, Damir Kronic¹, Gabriela O. Paiva-Silva⁵, Clothilde Pénalva⁴, Aurelio A. Teleman^{1,3,*}, Bruce A. Edgar^{1,2,4,*}

¹German Cancer Research Center (DKFZ), 69120 Heidelberg, Germany

²Zentrum für Molekulare Biologie der Universität Heidelberg (ZMBH), 69120 Heidelberg, Germany

³Heidelberg University, 69120 Heidelberg, Germany

⁴Huntsman Cancer Institute, University of Utah, Salt Lake City UT 84112 USA

⁵Instituto de Bioquímica Médica Leopoldo de Meis, Universidade Federal do Rio de Janeiro, Rio de Janeiro, Brazil.

Abstract

Sexual dimorphism arises from genetic differences between male and female cells, and from systemic hormonal differences^{1–3}. How sex hormones affect non-reproductive organs is poorly understood, yet highly health-relevant given the sex-biased incidence of most diseases⁴. Here we report that steroid signaling from the *Drosophila* ovaries to the gut promotes growth of the intestine specifically in mated females, enhancing their reproductive output. The fly's active ovaries produce the steroid hormone ecdysone, which stimulates intestinal stem cell (ISC) division and pool expansion in two distinct proliferative phases via its receptor EcR/Usp and downstream targets Broad, Eip75B and Hr3. Although ecdysone-dependent gut growth augments female fecundity, the more active, more numerous ISCs also increase female susceptibility to age-dependent gut dysplasia and tumorigenesis, potentially reducing lifespan. This work highlights the fitness trait trade-offs that occur when inter-organ signaling alters stem cell behavior to optimize organ size.

Users may view, print, copy, and download text and data-mine the content in such documents, for the purposes of academic research, subject always to the full Conditions of use:http://www.nature.com/authors/editorial_policies/license.html#terms

* correspondence: bruce.edgar@hci.utah.edu, a.teleman@dkfz-heidelberg.de.

AUTHOR CONTRIBUTIONS

S.M.A. performed and analyzed all experiments except ED Fig 8m, 9a–d (G.D.S.) and ED Fig 6a, e–q (C.P.). J.A.M. contributed to ED Fig 8a, n and Fig 2o. Conception and design of experiments by S.M.A, B.A.E., J.A.M., and A.A.T. Image processing methods designed by D.K. S.M.A., A.A.T. and B.A.E. wrote the manuscript.

COMPETING INTERESTS

The authors declare no competing interests.

DATA AVAILABILITY

The source data for all figures is available via the online Supplementary Information.

CODE AVAILABILITY

Code for all FIJI macros used in this study is available for download via the online Supplementary Information. These macros are available as Supplementary Data 1–6.

Keywords

Drosophila; ecdysone; steroid; gut; intestinal stem cell; nuclear receptor; hormone; inter-organ signaling; reproductive fitness; Eip75B; dysplasia; tumor

Steroidal sex hormones including estrogen, progesterone and testosterone regulate the growth and physiology of reproductive organs during puberty, the estrus cycle and pregnancy. Consequently these hormones also promote tumorigenesis in the breast, uterus, and prostate. Although sex-specific differences in physiology and disease predisposition extend to nearly all organs⁴, the functions of sex-specific steroids in non-sex organs remain relatively poorly explored and controversial. *Drosophila* utilizes one major steroid hormone, 20-hydroxy-ecdysone (ecdysone, 20HE) and its derivatives^{5,6}. Like vertebrate steroids, 20HE is synthesized by Cytochrome P450 enzymes from cholesterol. The ecdysone receptor comprises a ligand-binding *EcR* subunit and a DNA-binding subunit *Ultraspiracle (Usp)*, orthologs of human Farnesoid X and Liver X Receptors (FXR, LXR), and Retinoid X Receptor (RXR) respectively. In juvenile insects 20HE regulates developmental transitions including molting, metamorphosis, and sexual maturation. In adult *Drosophila* 20HE is made by the ovaries after mating, giving females higher levels than males^{3,5,7}. It acts in the adult nervous and reproductive systems^{3,8} affecting metabolism and lifespan^{9,10}, but a role in the gut has not been described.

Drosophila intestinal stem cells (ISC) are more proliferative in females than males, and females are more prone to age-dependent gut dysplasia and intestinal tumors^{2,11,12}. These sex-specific traits could be due to ISC-autonomous and/or systemic factors. Consistent with the former, stress-dependent ISC divisions, which are more frequent in females than males² (ED Fig. 1a, b), are reduced if the ISCs are masculinized by repressing the sex-determination genes *sxl* or *tra*² (Fig. 1a, ED Fig. 1b). Mated females support more ISC division than virgins (ED Fig. 1a–c), suggesting hormonal influences. Since mated females have higher ecdysteroid titers than virgins or males^{3,5,7}, we tested whether 20HE might affect ISC proliferation. Indeed, feeding virgin females 5mM 20HE strongly induced ISC divisions. This effect was independent of ISC sex identity (Fig. 1a, ED Fig. 1d), and also occurred in mated females and males (Fig. 1b–d, ED Fig. 1a). Using receptor-activity reporters, we confirmed that exogenous 20HE promotes *EcR/Usp* signaling in midgut ISCs, transient progenitors called enteroblasts (EB) and differentiated absorptive enterocytes (EC) (ED Fig. 1f–j).

20HE feeding, unlike detergent stress, induced two successive waves of ISC division (Fig. 1d, ED Fig. 1e). Using RNAi under the control of conditional cell type-specific *Gal4* drivers, we found that the first wave (at 6h post-20HE feeding) required *EcR* only in ISCs (Fig. 1e), but that later divisions (at 16h) also depended partially on *EcR* in EBs (Fig. 1e, ED Fig. 2a–f). Neither wave of division required *EcR* in ECs, enteroendocrine (EE) or neural cells (ED Fig. 2g–i). Isoform-specific tests revealed that *EcR-A* was much more important than *EcR-B* for the 20HE-induced division of ISCs (ED Fig. 2k–m). 20HE-induced divisions were reversible (ED Fig. 2j), suggesting a lack of toxicity. *EcR* activity was not induced by enteric infection (ED Fig. 1f–h), and *EcR* was dispensable for infection-induced gut regeneration

(Fig. 1h, ED Figs. 2a, k-l, n-q), implying a distinct role for EcR in the gut. Loss of *Usp*, however, did block infection-induced ISC divisions, suggesting that *Usp* has EcR-independent functions (Fig. 1h, ED Fig. 2a, n, p).

Next we asked whether ISC activation by 20HE involves *Upd*-*Jak*-*Stat* or *Egfr*-*Erk* signaling, pathways known to activate ISCs upon stress^{11,13}. Six hours of 20HE feeding induced the EGFR ligands *spi* and *krm* and their activating protease *rhomboid* (*rho*), but not the *upd2* or *upd3* cytokines or *Stat* signaling (ED Fig. 3a, b). Exposure to 20HE for 16h, however, moderately induced *upd2*, *upd3*, and *Stat* activity (ED Fig. 3c–h). Induction of *upd2*, *upd3*, and *rho* required EcR in ISCs and EBs (*i.e.* “progenitors”), though not in ECs (ED Fig. 3c–e). The EGFR effector, ERK, was also mildly activated by 16h of 20HE exposure, mostly in progenitors but occasionally in ECs (ED Fig. 3i). ERK activation required *upd2* (ED Fig. 3i), suggesting a signaling relay^{13,14}. Notably, the induction of all these targets (*upd2*, *upd3*, *Socs36A*, *rho*, *spi*, *krm*) by 20HE was suppressed by blocking ISC mitoses with RNAi’s targeting *string* (*stg*, *Cdc25*) or EGFR (ED Fig. 3f). This suggests that the observed increases in *Jak*-*Stat* and *Egfr*-*Erk* signaling are responses to epithelial stress from the early ISC divisions (see¹⁴). In further tests we found that *Upd2* from EBs and ECs contributed strongly to ISC divisions 16h after 20HE feeding, but only weakly to the early divisions at 6h (Fig. 1g; ED Fig. 3j–l). EGFR and *Rho*, however, were always required (Fig. 1f, ED Fig. 3j–m). We conclude that ISC divisions are initially activated ISC-autonomously via EcR, and require EGFR and *Rho*, whereas later divisions depend in part on cytokines produced in EBs and ECs, perhaps in response to stress from the first mitoses. The relationship of EcR to EGFR signaling begs further investigation.

Since mated females produce more ecdysone than virgins or males^{3,5,7}, we tested whether 20HE might account for sex-specific differences in the gut. Consistent with this, long-term exposure of males to 20HE phenocopied the female condition, increasing ISC mitoses, stress responsiveness, epithelial turnover, and midgut size (Fig. 1i–k, ED Fig. 4a–c). Genetically feminizing the male ISCs did not give these effects (Fig. 1j), suggesting that 20HE acts independently of genetic sex determination. Forced expression of *sSpi*, an ISC mitogen¹³ also failed to enlarge male midguts (Fig. 1j), implying that 20HE affects more than just ISC mitotic rate. Long-term 20HE feeding also endowed ISCs in virgin females with proliferative characteristics similar to those seen after mating (ED Fig. 4d). Conversely, RNAi’s that antagonized 20HE signaling in ISCs and EBs decreased gut size in mated females and suppressed mitoses in response to detergent stress (Fig. 2c, d, ED Fig. 4e–g). Thus, sexually dimorphic ISC proliferative traits are determined in part by 20HE signaling.

Ecdysone, like human estrogen and progesterone, promotes behavioral and metabolic changes that enhance female reproduction^{3,7,8}. Dose-response assays showed that 1mM 20HE fed to virgin females activated EcR targets, and ISC mitoses, to levels similar to mating (Fig. 2l, ED Fig. 5a). Hence we tested whether endogenous, mating-induced 20HE activates ISCs. Indeed, mating induced a large, transient increase in ISC division and enduring gut enlargement¹⁵ (Fig. 2a–d, ED Fig. 5 b–h, k). This was independent of genetic sexual identity (Fig. 2e, ED Fig. 5i). As with exogenously fed 20HE, these effects initially required EcR only in ISCs, though EcR in EBs contributed later on (Fig. 2f, g, ED Fig. 5e–

j). Like exogenous 20HE, mating also induced *upd2* and *rho* expression (ED Fig. 5l), suggesting that these are normal physiological responses.

To confirm the source of endogenous ecdysone, we used ovary-specific *Gal4* drivers^{3,7} to express RNAi's targeting the ecdysone synthesis enzymes *dib* or *spo*. This suppressed mating-induced ISC divisions and midgut growth, both of which could be restored by exogenous 20HE (Fig. 2h, j, ED Fig. 5n–p). *spo* mutants¹⁶ also failed to re-size the midgut after mating (Fig. 2i, ED Fig. 5m), confirming these results. To learn how the gut grows in mated females, we investigated effects on cell size and number. Depleting EcR in ECs did not reduce EC size (ED Fig 5q), but mating caused a large 20HE- and EcR-dependent increase in female ISC numbers (Fig. 2k, ED Fig. 5r–t). This expansion of the stem cell pool could cause an increase in total midgut cell numbers. These results imply that mating-dependent ISC division, ISC expansion, and gut growth are driven by 20HE signaling from the ovaries to progenitor cells in the gut.

Gut growth after mating is expected to increase intestinal nutrient absorption and nutrient supply to other organs. Since egg production is limited by nutrient availability to the ovaries, we tested whether 20HE-dependent gut growth affected female fecundity. When we blocked gut re-sizing by expressing *EcR^{RNAi}* in midgut ISCs, or in both ISCs and EBs, egg production was reduced by ~40% (Fig. 2p, ED Fig. 6b–d; see also⁷). This suggests that 20HE-dependent gut remodeling maximizes female reproductive fitness. However, we also noticed that our *Gal4* drivers were active in a small number of escort cells in the germarium of the ovary (ED Fig. 6a, e–l), raising the possibility that these fecundity defects were due in part to a requirement for EcR in those cells.

A study of *Drosophila* Juvenile Hormone (JH), a sesquiterpenoid, came to conclusions similar to ours, namely that JH promotes mating-dependent gut growth and fecundity in females¹⁵. We therefore investigated the relative roles of 20HE and JH. We found that the JH receptors *gce* and *met* are essential for ISC divisions in response to not only the JH receptor agonist, methoprene¹⁵, but also to 20HE and infection (ED Fig 7a–c). We confirmed the mitogenic effects of methoprene, but these were weaker than those of 20HE (ED Fig 7a–g, 5a), or mating (Fig 2a). Further, we discovered that methoprene-stimulated divisions require 20HE (ED Fig 7g), and that JH or methoprene could suppress ISC divisions driven by 20HE or other stimuli (ED Fig. 7a, d–f). While these results imply interplay between 20HE and JH, further work is required to elucidate their precise physiological relationship (see Supplementary Discussion).

To better understand how ecdysone activates ISCs we tested two known EcR targets: the transcription factor Broad, and the nuclear receptor Eip75B, a homolog of human Rev-Erb¹⁷. *Eip75B* and *Broad* mRNA were induced in midguts by 20HE or mating (Fig. 2l, ED Fig 8a), and progenitor cell-specific depletion of either factor suppressed 20HE-induced mitoses (Fig 2m, ED Fig. 8b–e). ISC clonal growth, however, required *Eip75B* but not *Broad* (ED Fig. 2b–c, 8e, f), highlighting Eip75B as a more essential effector. Eip75B overexpression was sufficient to promote ISC division and gut epithelial turnover (Fig. 2n, ED Fig 8g), whereas Eip75B loss impaired both ISC mitoses and maintenance (ED Fig 5s, 8c, f, h–i). Progenitor-specific Eip75B loss also blocked gut growth after mating (Fig. 2c),

and compromised egg production (Fig. 2p, ED Fig. 6b–d), phenocopying the effects of *EcR* loss. *Eip75B* binds DNA to repress target genes, and also binds the nuclear receptor *Hr3* to inhibit *Hr3*-mediated transcriptional activation¹⁸. Consistent with this mechanism, *Eip75B* overexpression or 20HE feeding suppressed an *Hr3* activity reporter, and *Hr3* overexpression suppressed ISC proliferation (ED Fig. 8j–l). Moreover, *Hr3* depletion counteracted losses in ISC proliferation caused by *Eip75B* depletion (Fig. 2o, ED Fig. 8n). While these results indicate that *Hr3* is a critical *Eip75B* effector, *Hr3* loss was not sufficient to activate ISC division (ED Fig. 8m–n), implying that *Eip75B* has additional targets. Further tests revealed that *Eip75B* and *Hr3* mediate 20HE-independent ISC responses to stress. Enteric infection strongly induced *Eip75B* mRNA (ED Fig. 8a) and suppressed *Hr3* activity (ED Fig. 8j). Removing *Eip75B* or *Broad* from ISCs by mutation (ED Fig. 2b–c, 8e) or RNAi (ED Fig. 8b–c, h–i, 9a–d) blocked infection-induced ISC mitoses, as did overexpressing *Hr3* (ED Fig. 9e). *Eip75B* was also required for ISC mitoses in response to the oxidative stress agent, paraquat (ED Fig. 8h–i). Further, we obtained evidence consistent with previous work¹⁷, that *Eip75B* action is modulated by Heme (*Eip75B* ligand) and Nitric Oxide (NO) (Fig. 2m, ED Fig. 9f–g). Functions for Heme and NO in the fly gut are unknown, but potentially interesting. We conclude that *Eip75B*, *Broad* and *Hr3* integrate multiple inputs in addition to 20HE to control ISC proliferation (ED Fig. 9h).

As females age, they experience progressive gut dysplasia wherein ISCs over-proliferate and mis-differentiate, leading to high microbiota loads (dysbiosis), barrier breakdown, and decreased lifespan^{19,20}. Age-dependent intestinal dysplasia is more pronounced in females than males¹², and can be identified by increases in mitoses and mis-differentiated cells doubly positive for ISC and EC markers. Suppressing *EcR*, *Usp*, or *Eip75B* in midgut progenitors significantly reduced both parameters of dysplasia in aged flies (Fig. 3a–c, ED Fig. 10a). Similarly, suppressing ecdysone synthesis enzymes (*dib*, *spo*) in the ovaries, or ubiquitously, also curtailed age-dependent gut dysplasia (Fig. 3d, ED Fig 10b–c). This effect could be reversed by 20HE supplementation. These results indicate that age-dependent gut dysplasia is potentiated by ovary-derived ecdysone, explaining the sex-bias of this condition.

Female *Drosophila* are known to be more susceptible than males to genetically induced ISC-derived tumors. We found that ISC/EB-specific RNAi targeting *Notch*, a receptor required for EC differentiation, drove tumor induction in 100% of mated females but was far less tumorigenic in males (Fig. 3e–g, ED Fig. 10d–e). Three results imply that this tumor predisposition is modulated by 20HE. First, in contrast to mated females, virgins were extremely resistant to *Notch*^{RNAi}-mediated tumorigenesis (Fig. 3e–h). Second, targeting 20HE signaling in ISCs with a dominant negative *EcR-A* inhibited tumor growth in mated females (Fig. 3e, g, ED Fig. 10d). Third, supplementing males or virgin females with 20HE increased tumor initiation and growth (Fig. 3g, h, ED Fig. 10f). We surmise that the utilization of mating-dependent, ovary-derived 20HE to stimulate gut re-sizing comes at a cost: it predisposes females to gut dysplasia and tumorigenesis (Fig. 3i, ED Fig 9i).

Gut dysplasia, tumorigenesis and egg production can all shorten lifespan^{10,20,21}, suggesting that the effects of ecdysone on the gut might adversely affect longevity. In fact earlier reports showed that *EcR* mutants live longer⁹, and proposed that reproduction can shorten lifespan by damaging the soma²². Our own lifespan assays, though subject to the same caveats as

others²⁰ (see Supplementary Discussion) support this view: suppression of EcR in midgut progenitors extended lifespan in females but not males (ED Fig. 10 g–i). In evolutionary terms, the disadvantage of a slightly shorter lifespan due to sex-specific hormonal signaling is probably insignificant relative to the reproductive fitness advantage conferred by increased egg production. This may be especially true in the wild, where gut dysplasia-dependent mortality is likely counteracted by nutrient deprivation¹².

Similarities in the reproductive biology of *Drosophila*^{3,8} and mammals²³ suggest that these inter-organ relationships have relevance to human biology. The mitogenic effects of insect ecdysone parallel those of estrogen and testosterone as drivers of breast, uterine and prostate growth and tumorigenesis. Yet how these steroids affect the human intestine remains poorly explored. Adaptive growth of the intestine is well documented in pregnant and lactating mammals²⁴, and might depend upon estrogen and/or progesterone. Laboratory tests with rodents and human cells, as well as some human subjects studies, have linked estrogen, testosterone, and their receptors to gastrointestinal cancers (*e.g.*²⁵), but epidemiological studies provide conflicting evidence regarding this association^{26,27} (see Supplementary Discussion). The contributions of sex steroids to intestinal physiology deserve more detailed study.

METHODS

Drosophila stocks and cultures

Drosophila melanogaster were raised on standard media and maintained in incubators with controlled temperature and humidity on a 12 hr light/dark cycle. Flies were transferred to fresh vials every 2 days. Male and female *Drosophila* were raised mated for all experiments, unless otherwise indicated. To generate controls, *w*¹¹¹⁸ (VDRC #60000) flies were typically outcrossed to the appropriate *Gal4* driver line. To generate controls for experiments using VDRC “KK” RNAi lines, the stock *y w*[1118]; *P*{attP,y[+],w[3']} (VDRC #60100) was outcrossed to the appropriate *Gal4* driver line. Full genotypes of all stocks used, and for each figure panel, are listed in Supplementary Tables 1 and 2.

Drosophila husbandry

For transgene expression using the *Gal4/Gal80^{ts}* system, experimental crosses were maintained at 18°C (permissive temperature for *GAL80^{ts}*) in standard medium. Animals of the desired sex and genotype were collected within 48h of eclosion and aged for an average of 5 days before shifting to 29°C (restrictive temperature for *GAL80^{ts}*) to induce UAS transgene expression. Adult midguts were dissected after different periods of time as indicated in on top of each figure panel. The *eSG-Flip-Out* system (*eSGF/O^{ts}*)²⁹ and the MARCM system³¹ were used to generate ISC-derived clones. Flies were aged for 3–6 days after eclosion before clonal induction by temperature shift to 29°C for *eSG-FO* clones or heat-shock for MARCM clones. Additional details on transgene expression times are indicated in the corresponding figure legends. MARCM 80B flies were heat shocked for 45–60 min in a 37°C water bath, and then aged for 12 days at 29°C before overnight treatment with vehicle, 5mM 20HE or *Psuedomonas entomophila* (*Pe.*).

Mating experiments

At least 10–15 virgin females for each genotype were collected at 18°C as they emerged. They were aged for ~5 days and then shifted to 29°C until the time points indicated in each figure panel. At the start of mating, females were transferred to fresh vials and allowed to mate with equal numbers of adult 3–7 days old wild type w^{1118} males, devoid of any transgenes, at 25°C, for optimal fecundity. Time when males were introduced to females in the same vial is denoted as t_0 . If indicated as mated once, then after 18–20 hours, the males were removed and the females were flipped into fresh vials every 48 hours until the indicated time in the respective figure panels. Otherwise, males were left together with the females for the following time points: 24 hours, 37–40 hours, 46–48 hours or 72–74 hours.

GAL4-LBD ‘ligand sensor’ system

Adult flies with bipartite detection system consisting of the LBD of the *Drosophila* nuclear receptor (NR) fused to the DNA-binding domain of yeast GAL4, along with a GAL4 UAS-controlled GFP reporter gene were used as previously described^{32,33}. Flies were raised and maintained at 25°C. For visualization of ligand sensor patterns, 5–7 day-old mated females were starved for 2–4h, heat-treated for 30 min in a 37°C water bath only once for EcR, Usp and Hr3 reporters, and allowed to recover at room temperature for 15 minutes. Then, flies were transferred to vials containing a fresh feeding vial (see Feeding Experiments) and kept at 25 °C for 16–18 hrs until dissection.

In vivo 10XSTAT92E-GFP reporter system:

Adult mated female flies of the genetic background 10XSTAT92E-GFP that have 10 Stat92E binding sites driving GFP expression were aged for 5–7 days and treated for 6hrs with 5mM 20HE and for 16–18 hrs with 5mM 20HE or *Pe*. infection.

In vivo Upd3 lacZ reporter:

Adult mated female flies of the genetic background Upd3.1 LacZ/TM6B were aged for 5–7 days and treated for 16–18 hrs with 5mM 20HE or *Pe*. infection.

Overnight Feeding Experiments

For all experiments except 20HE/SDS feeding (as indicated in the fig panel), flies were fed for 16–20 hrs, then dissected to remove the intestines, which were analyzed using immunofluorescence and confocal imaging. For timed 20HE feeding, flies were harvested as early as 4 hrs and as late as 22 hrs after continuous 20HE exposure. We observed a window of strong mitotic response at 6 hrs and again at 16–18 hrs that persisted to 22 hrs after exposing the flies to the 20HE feeding solution.

For 20HE removal experiments, flies were fed overnight (O/N) for 16–18hrs with 5mM 20HE, and then transferred to a fresh vial for another O/N treatment after which the midguts were dissected and stained.

20-hydroxy-ecdysone (20HE) feeding: 10–15 adult male, mated female, or virgin female flies were used for the ecdysone feeding experiments, as indicated. 20HE was weighed out of the supplier’s vial and was first dissolved in 100% ethanol. Water was then added to make

up a 25mM stock solution in 10% ethanol. 25mM 20HE stocks were stored at -20°C . A final concentration of 0.25–10 mM ecdysone or 2% ethanol (as control) was used for the feeding experiments as indicated. 200 μL of 5% sucrose solution, 5 mg/ 1mL dry yeast + 5mM 20HE (Sigma-Aldrich H5142) mix was deposited on top of a standard food vial to which flies were transferred. If the experiment required *Pe.* infection, then 400 μL of the same yeast/sucrose mix (described above) was deposited on filter-paper discs (Whatmann) to which flies were being transferred. The sucrose yeast mix with 2% ethanol was used as vehicle treatment.

Detergent treatment: flies were left to feed on yeast sucrose solution (described above) with 0.1% or 1% SDS for 18–20h or at the times indicated.

Enteric *Pe.* infection: A 25 mL pre-culture was started the first day by inoculating *Pseudomonas entomophila* (*Pe.*) bacteria from glycerol stocks (stored at -80°C) in Rifampicin-supplemented Luria Broth (LB; final antibiotic concentration: 100 $\mu\text{g}/\text{mL}$). The pre-culture was grown overnight at 29°C , shaking at 130 rpm. Next day, the pre-culture was diluted in 175 mL Rifampicin supplemented LB and the culture was again grown overnight at 29°C , shaking at 130 rpm. After the growth of the bacterial culture reached optical density (O.D) ≈ 0.5 , the culture was spun down at 2500 g for 25 min at 4°C and the pellet was re-suspended in 3 mL of 5% sucrose + 150 μL yeast. Prior to infection, flies were starved for 2 hrs (optional step), and then placed in vials with 500 μL of this *Pe.* solution or 5% sucrose with yeast as the control vehicle.

Other treatments in Fig 3 and ED Fig 8, 9 include feeding with 2.5mM Paraquat, $\text{N}\omega$ -Nitro-L-arginine methyl ester hydrochloride (Sigma-Aldrich, N5751) (200 mM L-NAME stock solution in distilled water; final 10mM concentration was used), (\pm)-S-Nitroso-N-acetylpenicillamine (Sigma-Aldrich, N3398) (500 mM SNAP stock solution in 10% ethanol and 10mM SNAP final solution was used), Hemin (Frontier Scientific, H651–9) (2 mM stock solution dissolved in 0.1M NaOH, pH adjusted to 7 with sodium phosphate buffer and 0.5 mM final solution was immediately used) and their corresponding vehicle. Treatments were diluted in 400 μL total volume of 5% sucrose and 5 mg/1 mL yeast then added vials containing a fresh feeding paper.

Long term ecdysone feeding

At least 10–15 adult male and/or female flies were transferred to standard fresh food vials (2.5 cm diameter) containing circa 3 mL of food. To prepare ecdysone treated food, the food in the vial was scraped on the surface and 200 μL 1mM 20HE, 22 mg/mL yeast in 5% sucrose solution was added. After 15 minutes, this solution diffused into the food. Flies were added to these vials and flipped into fresh 20HE containing vials every 48 hrs for 14 days unless otherwise indicated. As vehicle, vials with fly media containing 200 μL 0.43% ethanol in sucrose/yeast solution were used. Flies were dissected to remove the intestines, which were analyzed using immunofluorescence and confocal imaging. For the flies raised on low nutrient food, flies were fed with 1mM 20HE, 5 mg/mL yeast in 5% sucrose solution that was deposited on filter-paper discs (Whatmann) and exchanged every 24–30 hrs. For *Pe.* infection after long-term 20HE feeding in ED Fig 4c, we discontinued feeding the flies

on ecdysone-containing food for one day before the flies were fed with the *P.e.* bacterial solution.

Fecundity assays

Fig 2p, ED Fig. 6b: Ten-15 virgin females for each genotype/replicate were collected at 18°C as they eclosed, and pooled in one vial. For each genotype 3–4 replicates were performed for every experiment. Virgins were aged one day and then shifted to 29°C to activate Gal4. Females were then transferred to fresh cages and allowed to mate with equal numbers of *w*¹¹¹⁸ males. Females were housed in groups of 7–10 with equal number of males for this experiment. Standard *Drosophila* media was poured in 5 cm plates and stored at 4°C. Flies in each egg collection cage were flipped onto fresh food plates every 24–48 hours for the indicated number of days, and the number of eggs/replicate were scored and averaged over the number of flies in each cage. Three-four independent experiments were performed, all results were pooled, and are shown in the Fig 2p and ED Fig 6b. Raw egg counts, processed cumulative sums, averages, and p-values for every experiment are available in the online source data.

ED Fig. 6d: Virgins were aged 8 days at shifted 29°C to activate Gal4 first before mating to equal number of males. Females were housed in groups of 7–10 with equal number of males for this experiment. Flies in each egg collection cage were flipped onto fresh food plates every 24–48 hours for the indicated number of days, the number of eggs/replicate were scored and averaged over the number of flies in each cage. Cages with dead flies were excluded from the analysis. Raw egg counts; processed sums and p-values are available in the online source data.

ED Fig. 6c, d: Virgins were aged one day and then shifted to 29°C to activate Gal4. Females were then transferred to fresh vials and allowed to mate with equal numbers of *w*¹¹¹⁸ males. All subjects were housed overnight in the same vial to ensure mating success and numbers of eggs were counted and averaged for the number of females/vial. Next day, every female/male pair was separated and individual female/vial were followed up for 14 days. Vials were exchanged every 24–48 hours in this experiment and total number of eggs laid/2 days was counted for every female fly. Vials with dead flies were excluded from the analysis. Raw egg counts; processed cumulative sums/averages and p-values are available in the online source data.

A 2- or 3-day sum was calculated from the average number of eggs/fly laid every day, then an average sum of eggs laid/fly/3 days across the replicates was plotted with error bars \pm confidence intervals (c.i.). Alternatively, the average/individual cumulative numbers of eggs were summed up and mean values were plotted with error bars \pm standard deviation (s.d.). To test statistical significance for each day, Two-sample unequal variance t-test were performed, with a two-tailed distribution assuming unequal variance for test genotype relative to control at every time point. Individual p-values are available in the online source data. Alternatively for Fig 2p, general linear models (GLMs) with binomial errors were used to examine the effect of the genotype on the average cumulative number of eggs.

spo mutant rescue experiment

Males of either deficiency backgrounds BM#7584 or BM#24411 were crossed to heterozygous *spo* mutant virgins and allowed to lay eggs on apple plates for several days prior to the experiment. 2 deficiency genotypes were used to increase the likelihood to getting rescued homozygous *spo* mutant flies. On the day of the experiment, the parents were left to lay eggs for 4 hours then, were removed. The eggs were allowed to age 4–6 hours at 25°C then, were all pooled in a sieve and de-chorionated by bleach. After washing in PBS-T, the de-chorionated embryos were incubated in PBS-T supplemented with 100 μ M 20E for 3 hours. The embryos were covered with Halocarbon 27 Oil and incubated at 18°C overnight. *Over the next 2 days*, homozygous *spo* embryos were selected under a fluorescent stereoscope by the lack of GFP expression in the hatched larvae. The phenotypically correct larvae were collected in fresh food vials at the density of 40–60 larvae/vial and allowed to develop at 25°C until eclosion and selection of virgin or mated homozygous *spo* mutant flies.

Lifespan assays

Males and females of the genotype 5961GS EcR A DN were allowed to mate for 48hrs then were isolated in groups of 25 flies of the same sex/vial. For RU486 food supplementation, 100 μ l of a 5 mg/ml solution of RU486 or vehicle (ethanol 80%) were deposited on top of a food vial and dried for at least 4–6 hours, resulting in a 0.2 mg/ml concentration of RU486 in the food accessible to flies. Flies were flipped every 48hrs into a fresh vial. Dead flies were visually identified (flies not moving, not responding to mechanical stimulation and laying on their side or back were deemed dead), and the number of dead flies was recorded. Oasis software was used for data analysis³⁴. Log rank non-parametric test was performed by the software and the *P* values were derived from pairwise comparison with Bonferroni correction as displayed in ED 10 g-h.

Immunohistochemistry and microscopy

Drosophila adult midguts were dissected in 1 \times phosphate-buffered saline (PBS) and fixed with 4% paraformaldehyde for 30 min at room temperature (RT). For all immune-stainings except anti-dpErk, samples were washed with 0.015% Triton-X in PBS thrice at RT, then permeabilized with 0.15% Triton-X in PBS for 15 min at RT with shaking. Then, samples were re-washed and blocked in PBS with 2.5% BSA, 10% normal goat serum and 0.1% Tween-20 (blocking solution) for at least 1hr at RT. Midguts were incubated with primary antibody at 4 °C overnight at the following dilutions: chicken anti-GFP (Life Technologies/Molecular probes, 1:500); rabbit anti-phospho-Histone 3 (Merck Millipore 1:1000); mouse anti-phospho-Histone 3 (Cell Signaling, 1:1000); guinea pig anti-GFP (Teleman Lab, 1:1000); chicken anti- β -galactosidase (Abcam, 1:1000).

For the dpErk detection, samples were fixed in 4% paraformaldehyde, dehydrated for 5 min in 50%, 75%, 87.5%, and 100% methanol, and rehydrated for 5 min in 50%, 25%, and 12.5% methanol in PBST (0.1% Triton X-100 in 1 \times PBS). After washing in 1 \times PBST, midguts were blocked in PBS with 2.5% BSA, 10% normal goat serum and 0.1% Tween-20 (Blocking solution) for at least 1hr at RT then incubated with rabbit phospho-p44/42 MAPK (Erk1/2) (Thr202/Tyr204) #9101 (Cell Signaling, 1:400) at 4 °C overnight.

After washing, all samples were incubated with secondary antibodies (Alexa 488, 568 or 633, Invitrogen) >2 hours at RT at a dilution of 1:1000. All antibody incubations were performed in blocking solution. DNA was stained with 0.5 µg/mL DAPI (Sigma).

For the plasma membrane cell stain: Freshly dissected midguts were stained with CellMask™ deep red plasma membrane stain, Thermofisher® in 1× PBS at a concentration of 1:1000 then fixed in 4% formaldehyde and stained with 1× PBS/DAPI according to the manufacturer's instructions.

Ovary staining: One day old mated females have been place on active yeast paste for 4–5 days at 29°C. Ovary have been dissected in dPBS, transfer in PBS, PFA8% and fixed for 10min at room temperature under mixing. After washes in PBS triton 0.15% the ovaries have been blocked for 1 hour in PBST0.15%, BSA 2,5%. The primary antibodies incubated at 4°C overnight in blocking buffer: chicken anti-GFP 1/500, mouse anti-coracle 1/500 (http://dshb.biology.uiowa.edu/C566-9_2). Then the ovaries have been washed 5 times 5 minutes in PBS T0.15% and incubated 1h30 with the secondary antibodies +dyes in blocking buffer at room temperature: Goat anti-chicken488 1/1000, Goat anti- Mouse568 1/1000, Hoechst 1/1000, phalloidine633 1/10000. After two washes of 10min in PBST0.15%, the ovaries have been mounted between slide and coverslip in Vectashield. Images have been acquired using a Leica Sp8 confocal microscope and the figures made using Fiji with the ScientiFig plugin.

Imaging: Midguts were mounted on glass slides in VectaShield (Linaris®). All midgut images were acquired on a Leica TCS SP5II inverted confocal microscope, equipped with HCX Plan APO 20×/1.30 glycerol-immersion (for quantifications) or 40×/1.30 oil-immersion objectives (for representative images/ quantifications), using Leica Application Suite (LAS) AF software and processed with Fiji/ImageJ software³⁵. Representative images are shown. GFP, in green (native GFP for all genotypes except for the reporter midguts and *Su(H)*⁺ cells marked with *Su(H)*^S driver that were additionally stained with GFP for better visualization of the signal); DNA: DAPI, in blue. For displaying images in the figure panels, a Z-stack of defined steps for control and test genotypes in a single field was acquired in the R4 region (a region which is bounded by the apex of the midgut tube's most distal 180° turn) as described in³⁶. Images represent maximal intensity projections of the acquired Z-Stacks. Scale bars are 100 µm in all images, unless otherwise indicated.

Quantifications and statistics

ISC proliferation: Mitotic indices were determined by manually counting all PH3 positive cells in entire midguts using Leica DM5000B or Zeiss Axiophot fluorescence microscopes through a 40× objective. Statistical analysis of all the mitotic counts was performed using two-tailed Mann-Whitney test (ns $P > 0.05$, * $P < 0.05$, ** $P < 0.01$, *** $P < 0.001$, **** $P < 0.0001$). All dot plot graphs indicating mitoses are showing mean values ± s.d. Exact P values are provided in a table in the supplemental material. Data were plotted from at least 3 independent experiments.

Quantification of the GFP⁺/delta⁺ cells: Z-stacks of both epithelial sides in R4a/b region were imaged at steps of 5.0 µm at 40× then the total number of GFP⁺ or delta⁺ cells were

analyzed after limiting the particle size to 10–250 μm , circularity 0.00–1.00 and excluding holes after maximal Z-projects have been applied.

Quantification of the delta+ and Su(H)+ cells: Z-stacks of both epithelial sides in the R4a/b region were imaged by confocal Zeiss LSM 780 Spinning Disc. The total number of DAPI+, Su(H)+ and delta+ cells were automatically segmented and counted using a custom Image J/ FIJI macro (Supplementary Data 6). Su(H)+ and delta+ cells were manually recounted and verified and the numbers of each cell type were recorded to derive %cell type to total cell number/stack.

Quantification of cell size: Midguts were mounted as previously described and Z-stacks of both epithelial sides in the R4a/b were imaged at steps 5.0 μm at 40 \times then a custom Image J/ FIJI macro (Supplementary Data 1) was created to segment the cytoplasm in reference to DAPI nuclear stain and internuclear distances. Area of the cells in μm^2 were outputted to Microsoft Excel and a mixed effects 2-way ANOVA statistical model was computed to calculate the significance between the different conditions.

Quantification of clonal size: Z-stacks of both epithelial sides in the R4a/b were imaged at steps 5.0 μm at 40 \times then a custom Image J/FIJI macro (Supplementary Data 2) was used to semi-automatically segment and determine the location and size of the GFP+ clones then the sizes in μm^2 were outputted to Microsoft Excel and a mixed effects 2-way ANOVA statistical model was computed to calculate the significance between the different conditions.

Quantification of the GFP+ areas: For analysis of the mating effects, Z-stacks of both epithelial sides in R4a/b region were imaged at steps 5.0 μm either at 40 \times or at 20 \times s. For analysis, the quantification of the area occupied by GFP+ cells was performed automatically using a custom ImageJ/FIJI macro (Supplementary Data 3). The macro created maximum Z-Projection of image stacks, median and gaussian filtering, automatic thresholding and measurement of GFP+ and gut occupying area. The measurements were exported to Microsoft Excel and the GFP+ / gut area ratio was derived from these values for at least 10 midguts for most experiments.

Quantification of the GFP+ area/ DAPI+ cells: For analysis of the tumor effects (ED 10e), a fixed median filter was created for each stack, a fixed gaussian blur value was applied; then the midgut was thresholded for DAPI+ cells and GFP+ cells; then areas for both were calculated and a ratio was derived. An Image J/FIJI macro was used (Supplementary Data 3).

Data are displayed in scatter plots with the mean values \pm standard deviation (s.d.) for each series of experiments. Data shown are representative of at least 2–3 independent repeated experiments with similar results. Statistical significance was calculated either by two-tailed Mann-Whitney test without a multiple comparison test. Results were considered to be significantly different at $p < 0.05$. All calculations were performed using the Prism 7.0 software (GraphPad Software, La Jolla, CA, USA).

Gut measurements: After immunofluorescence staining and prior to mounting, midguts were put on a glass slide and imaged using a Leica M205 FA Stereo Microscope or Stereo Discovery.V8, unmounted guts were imaged at a defined magnification and these images were exported to Fiji for further analysis. Custom Image J/FIJI macros (Supplementary Data 4, 5) were used to threshold each image then measure the area of each midgut. With the distance mapping technique, the midgut length was derived. For the width measurements, a line was drawn. Before quantifying any midgut dimensions, the genotype of each sample was concealed. Samples were randomly analyzed then the genotype was revealed only after completing analysis. For statistical analyses of gut sizes, normality test was performed with Shapiro-Wilk normality test and the gut sizes showed normal Gaussian distribution. Thus, statistical significance of gut size measurements was calculated by ordinary ANOVA test, followed by Bonferroni's multiple comparisons test. *P* values were calculated as follows: (ns $P > 0.05$, * $P < 0.05$, ** $P < 0.01$, *** $P < 0.001$, **** $P < 0.0001$). Data are displayed in scatter plots with the mean values \pm standard deviation (s.d.). Data were plotted from at least 3 independent repeated experiments with similar results.

All Image J/FIJI macros are available as supplementary online source material (Supplementary Data 1–6), or upon request from the authors.

Sample sizes, Randomization, and Blinding

No statistical method was used to predetermine sample sizes, but typically between 5 and 20 flies were used per replicate per genotype in each experiment. Exact *n* values for each experiment can be found in the online source data. When selecting animals for an experiment, the parental genotype was not concealed because it was required to select pertinent progeny. Animals were first selected by genotype and then randomly chosen for experimental analysis. For measurements of mitoses/gut, gut sizes and tumor frequencies, the genotype of each sample was concealed during analysis. Samples were then randomly scored and genotypes were revealed only after completing the analysis.

RT-qPCR

10–12 female intestines per genotype were dissected and RNA isolated using the RNeasy kit (QIAGEN). 750 ng of total RNA was used for cDNA synthesis reactions using the QuantiTect reverse transcription kit (QIAGEN). RT-qPCR was performed on a Light Cycler 480 II (Roche) using SYBR Green I (Roche). Experiments were performed in at least biological triplicates. Relative fold differences in expression level of target genes were calculated as ratios to the mean of the reference genes *rp49* and *tubulin* using the $2^{-\Delta\Delta C_t}$ method. A series of 10-fold dilutions of an external standard was used in each run to produce a standard curve. Primer sequences are listed in the online Supplementary Table 3.

$2^{-\Delta\Delta C_t}$ method: $2^{-\Delta\Delta C_t}$ (or \log_2 fold change) is the difference in threshold cycles for the test and control sample normalized to the threshold cycles for the reference gene.

$$\Delta C_t = C_t (\text{test}) - C_t (\text{control})$$

$$2^{-\Delta\Delta C_t} (\text{test}) \text{ or } 2^{-\Delta\Delta C_t} (\text{control}) = 2^{-(C_t \text{ target gene} - C_t \text{ reference gene})}$$

All data are presented as mean fold change (\log_2) with s.d.

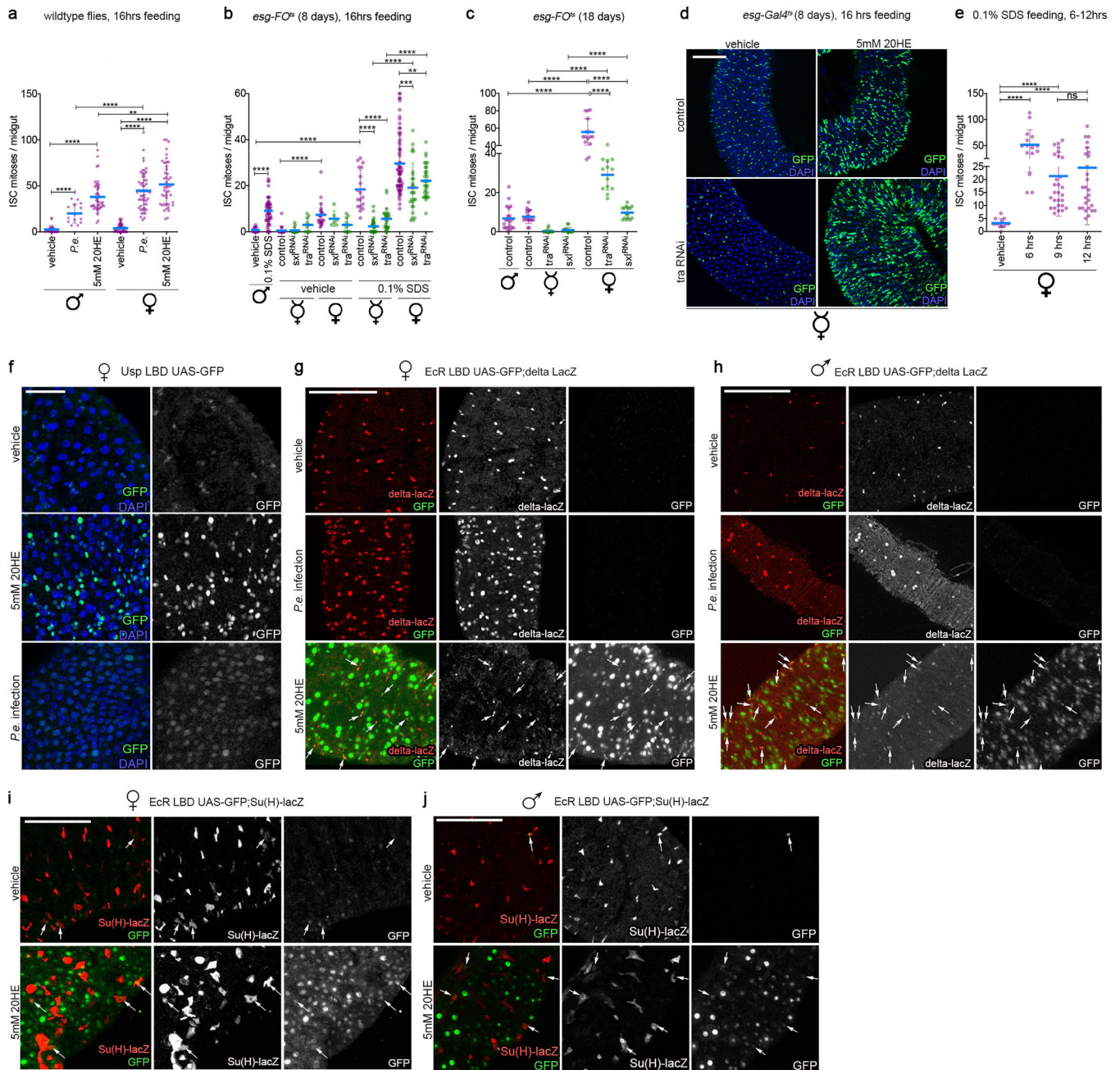
Extended Data

Author Manuscript

Author Manuscript

Author Manuscript

Author Manuscript



ED Fig. 1: 20HE feeding promotes sexually dimorphic ISC mitotic activity.

(a) Male ISCs do not divide strongly in response to infection elicited by pathogenic bacteria, but divide to a similar extent as mated female ISCs in response to 20HE feeding, quantified by counting the number of dividing ISCs per midgut using phospho-histone-3 staining (also termed mitotic index) in males and mated females after 16–18 hrs treatment with 5mM 20HE or pathogenic *P.e.* infection. Males are fully and equally competent to respond to 20HE treatment as mated females.

(b) Mating boosts the mitotic divisions of ISCs. Feeding 0.1% SDS for 16 hrs to virgin females induces ISCs mitoses and this is inhibited by masculinizing ISC clones using *sxl* or

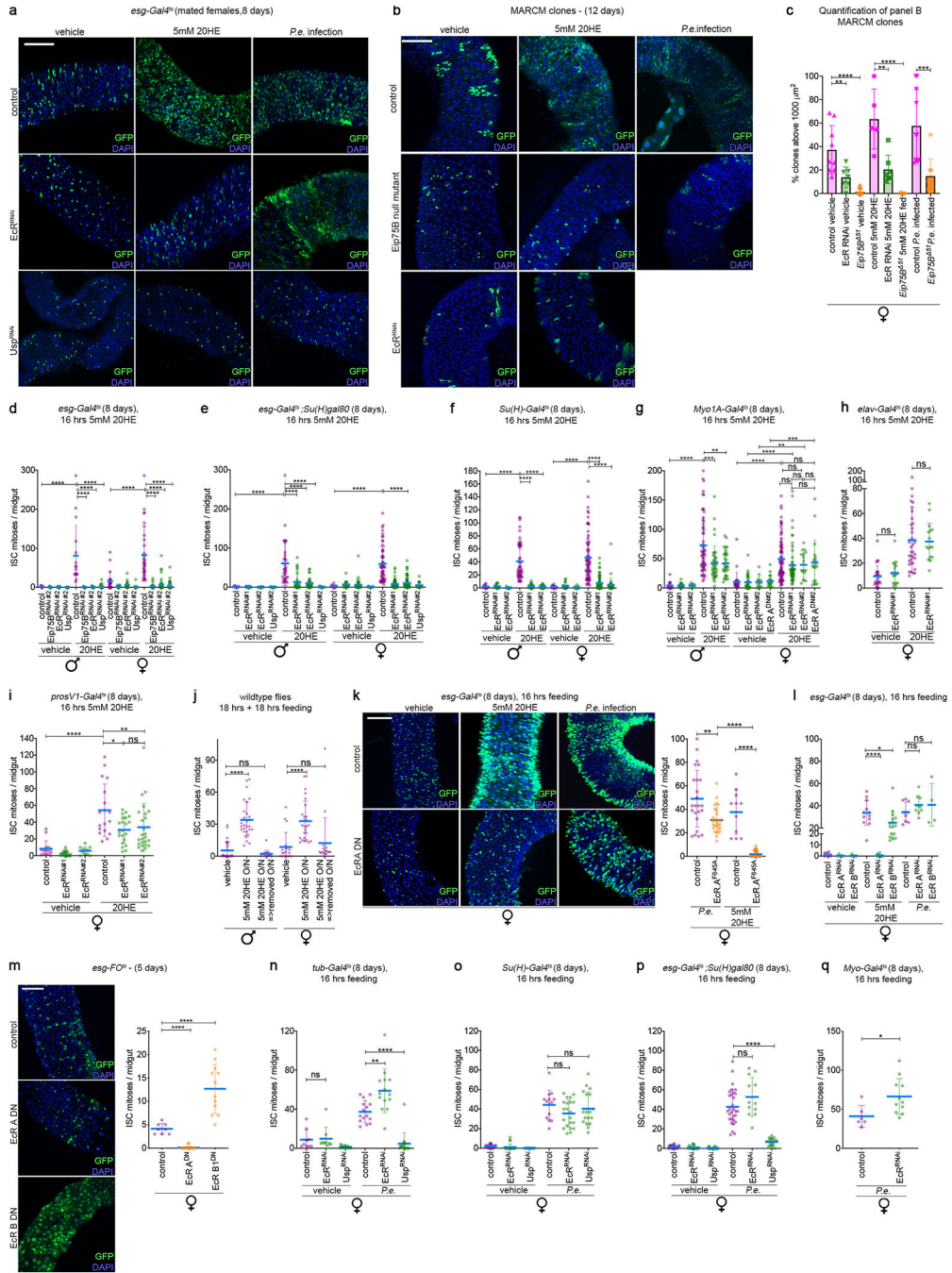
tra RNAi. Mating increases the ISC mitotic responses to SDS feeding and somewhat restores the ability to masculinized ISCs to divide to stress.

(c) Mating induces basal ISC mitoses in both female (control) ISCs and in masculinized ISC clones with tra or sxl depletion.

(d) 20HE feeding leads to the proliferation and expansion of both control ISCs and ISCs of tra^{RNAi} masculinized progenitors. Representative images are shown 16 hrs after 5mM 20HE feeding. This experiment was repeated 3 times with similar results. Quantification of this experiment is in main Fig 1a.

(e) Quantification of ISC division at different time points (6, 9 and 12h) after feeding 0.1% SDS to mated females.

(f-j) Males or mated females of the genotypes Gal4.DBD-Usp.LBD>GFP (Gal4-Usp>GFP) (panel f) or Gal4.DBD-EcR.LBD>GFP (Gal4-EcR>GFP) (panels g-j) were heat shocked for 30 min to induce expression of the ligand sensor system, and then either infected with *P.e.*, or fed with 5mM 20HE or vehicle and dissected 18–20hrs later. These GFP ligand traps express GFP under the control of heat-inducible promoter and mark cells with active 20HE signaling. When fed with vehicle, both Gal4-EcR>GFP and Gal4-Usp>GFP were expressed in a few cells in the R4 region posterior midgut (image shown) and in many more in the anterior midgut (image not shown). White arrows where applicable indicate cells that are double positive for delta or Su(H) lacZ markers. 5mM 20HE feeding caused a strong increase in GFP expression in the posterior midgut indicating an up-regulation in the activity of both reporters. GFP was expressed in many delta⁺ cells (panels g,h) and much fewer Su(H)⁺ (panels i,j) of both males and females upon 5mM 20HE feeding. The majority of the remaining positive cells are enterocytes. Upon 20 hrs of *P.e.* infection, GFP signal disappears from males and females guts indicating that EcR does not play a role in infection-induced stress response (panels g,h). However, Usp reporter was still active in many gut cells as a consequence of *P.e.* infection (panel f). Usp reporter was also positive in many cell doublets and bigger cells of the midgut. These reporter data suggest that EcR and Usp are both activated by exogenous 20HE feeding yet, they act differently in response to infection. Representative images are shown. This experiment was repeated 5 times with similar results. For all panels, control flies express UAS-GFP instead of the transgene. The period of RNAi induction is indicated above every panel. Results in dot plots are from 3 or more independent biological replicates. Center is the mean and error bars represent \pm s.d.. N 10 are plotted for each genotype in each scatter plot. Statistical analysis was performed using Mann-Whitney test with two-tailed distribution. (***P* 0.01,*** *P* 0.001, **** *P*<0.0001). Exact *n* numbers and *P* values >0.0001 can be found in the online source data. Representative images are shown. GFP, in green; DAPI, in blue; delta lacZ, in red (g-h); Su(H) lacZ, in red (i-j). Scale bars, panel f=50 μ m; panels d,g-j=100 μ m. The overnight standard period of feeding the flies was 16–20 hours. σ refers to males, \varnothing refers to virgins and φ refers to mated females.



ED Fig. 2: The second mitotic wave of 20HE requires EcR/Usp in progenitors while EcR is dispensable to ISCs in their response to *P.e.* infection. (a) Representative pictures of samples from the experiment presented in main Figures 1c and h. Both EcR and Usp are required in progenitors for the mitoses induced 16h after 20HE feeding, while only Usp is cell-autonomously required by the ISCs for *P.e.*-induced mitoses. Shown are images of progenitor accumulation after 20HE- or *P.e.* feeding to mated females. (b) ISCs depleted of EcR or its downstream target Eip75B fail to form clones in response to 20HE feeding. Eip75B null mutant clones also fail to regenerate the epithelium following

P.e. infection. EcR depleted or Eip75B null mutant clones were generated by MARCM and analyzed 12 days after clonal induction followed by 5mM 20HE feeding or *P.e.* infection for 16–18 hrs. Vehicle-fed control clones were multicellular and spread throughout the epithelium, whereas EcR depleted clones were considerably smaller, mostly between 2–4 cells, and rarely up to 10 small cells/clone. Eip75B null mutant clones remained mostly single ISC clones. After 16hrs of 20HE feeding, the epithelium is populated with newly formed cells within the control clones however, both EcR and Eip75B depleted clones remained unable to divide indicating the ISC cell autonomous requirement of EcR and Eip75B for ISC mitoses both basally and in response to exogenously fed 20HE. Similarly, after *P.e.* infection, GFP+ cells expanded in control clones, whereas Eip75B null mutant clones were considerably smaller.

(c) Quantification of panel B by a macro designed to assess clonal sizes/maximum Z projection. (see materials and methods, Supplementary Data 2).

(d) Both EcR and Usp are required in gut progenitor cells for the 20HE induced-mitotic response as shown by the reduced ISC mitotic activity 16 hrs after feeding 5mM 20HE to flies with progenitor-specific depletion of EcR or Usp in males and mated females. Results shown are for a 2nd RNAi line to complement the results in Fig 1c.

(e) EcR or Usp depletion in ISCs abolishes ISC mitoses 16 hours after feeding 5mM 20HE to males and mated females. Results shown are for 2 different RNAi lines.

(f) EcR is required in EBs for the 2nd wave of ISC mitoses induced 16 hrs after feeding 5mM 20HE to males and mated females. Results shown are for 2 different RNAi lines. This experiment indicates that in contrast to the 1st wave (see Fig 1e), EcR is required non-cell autonomously in EBs for 20HE induced ISC divisions.

(g) EcR is non-autonomously required in ECs for maximal induction of ISC mitoses in response to 20HE. The *Myo1A-Gal4^{ts}* driver (*Myo1A-Gal4 tub-Gal80^{ts}*) activates UAS target gene expression specifically in enterocytes (ECs). Results shown are for 2 different RNAi lines for both males and females, and for a dominant negative isoform of EcR in females.

(h) EcR in the nervous system is not required for intestinal 20HE-stem cell induced mitoses. EcR depletion was induced using *elav-Gal4 tub-Gal80^{ts}*, a pan-neuronal driver for the adult central nervous system. 16 hrs after 5mM 20HE feeding, ISCs mitoses were scored and midguts with EcR depletion in the CNS did not exhibit a change in their division rates in comparison to control females.

(i) EcR in enteroendocrine (EE) cells plays a minimal role in 20HE induced ISC mitoses of the midgut. Slightly compromised mitotic indexes in 20HE fed mated females upon EE-specific depletion of EcR in EEs using the EE-specific *prosV1-Gal4 tub-Gal80^{ts}* driver indicate that EcR in EEs is dispensable to the 20HE induced ISC mitoses. Results shown are for 2 different RNAi lines.

(j) 20HE only transiently induces ISC mitoses, quantified by mitotic indices of male and female wildtype flies subjected to 2-day of the indicated treatment regimes. ISC proliferation is restored to basal levels after 5mM 20HE was withdrawn, suggesting that 20HE's actions are not detrimental. Male and female flies were fed vehicle or 20HE in different successions such that flies were exposed for 20 hrs to the first treatment, then for another 24 hrs to the second treatment. ISC mitoses returned to basal levels after 16–20hrs treatment with 20HE then vehicle.

(k) Expression of an EcR-A dominant negative isoform inhibits the ISC proliferative response to 5mM 20HE but not to enteric infection. (Left) Images of progenitors marked with *esg-Gal4* following *Pe.* or 5mM 20HE feeding, indicative of ISC proliferation in control mated females. (Right) mitotic counts.

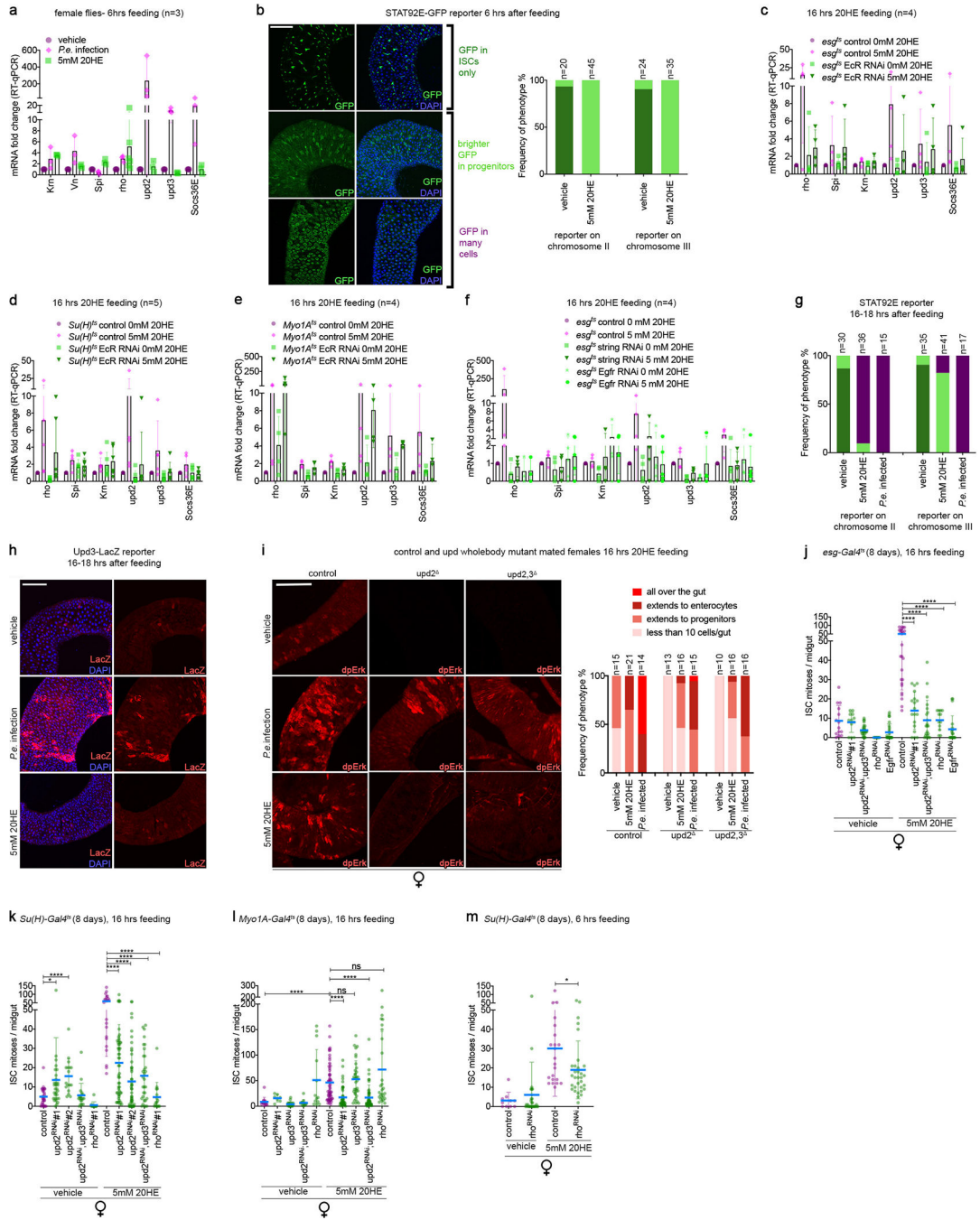
(l) 20HE signals mostly through isoform EcR-A to mediate ISC proliferation. Progenitor specific expression of *EcR-A^{RNAi}* and *EcR-B^{RNAi}* shows that EcR-A, more than EcR-B, is required in ISCs for their mitotic response 16–20 hrs after feeding of 20HE. Knockdown of neither EcR-A nor EcR-B had an effect on the *Pe.*-induced ISC mitoses.

(m) EcR isoform A is much more important than isoform B for driving the intestinal hyperplasia, as shown in images of posterior midguts of mated females expressing EcR A DN or EcR B DN. (Left) Images of clonal expansion under basal conditions at 5 days after induction of expression of different EcR dominant negative isoforms in mated female midguts. (Right) ISC mitotic counts.

(n-q) EcR in ISCs or other differentiated cells is not required for the *Pe.* induced mitotic response of ISCs, whereas Usp is cell-autonomously required by ISCs to proliferate in response to *Pe.* infection. Quantification of the mitotic indexes of ISCs following *Pe.* infection in mated females where EcR or Usp was depleted either (n) constitutively in all cells using the *tub-gal4^{ts}* driver, (o) in EBs, (p) in ISCs or (q) in ECs. Collectively, these experiments indicate a functional bifurcation of EcR and Usp, whereby Usp is essential in ISCs for the *Pe.*-induced ISC response. RNAi was induced in progenitors of mated females for 8 days before 16–20 hrs *Pe.* infection or 20HE feeding.

For all panels, control flies express UAS-GFP instead of the transgene. The period of RNAi induction is indicated above every panel. Results in dot plots are from 3 independent biological replicates. Center is the mean and error bars represent \pm s.d.. N = 10 are plotted for each genotype in each scatter plot. Statistical analyses were performed using Mann-Whitney test with two-tailed distribution. (**P* 0.05, ***P* 0.01, ****P* 0.001, *****P* < 0.0001). Exact *n* numbers and *P* values ≥ 0.0001 can be found in the online source data. Representative images are shown from experiments that were repeated 3 independent times. GFP, in green; DAPI, in blue. Scale bars, panels a,b,k,m=100 μ m.

The overnight standard period of feeding the flies was 16–20 hours. σ refers to males and f refers to mated females.



ED Fig. 3: The second mitotic wave of 20HE regulates Jak-Stat signaling and requires Egfr signaling in the midgut progenitors.

(a) Components of Egf signaling but not Jak-Stat pathway are transcriptionally induced 6 hrs post 20HE feeding. mRNA levels of Egf ligands such as keren, spitz and their cleaving protease rho are transcriptionally induced while unpaired cytokines upd2, upd3, Jak-Stat target Socs36E are not induced 6 hrs after 20HE (light green bars) relative to vehicle fed control females (dark pink bars). In contrast, *P.e.* infection causes a strong induction of JAK-STAT signaling components upd2, upd3, Socs36E as well as a milder upregulation of Egf

signaling components *keren*, *vein* and *rho* (light pink bars). Mated female midguts of wildtype flies were fed with vehicle, *P.e.* or 5mM 20HE for 6 hrs then expression levels in guts were determined by RT-qPCR. Expression is indicated as mean fold change relative to vehicle-treated midguts \pm s.d. (n=3).

(b) (Left) Representative images of 3 categories of activity for the phenotypes of STAT92E-GFP reporters on chromosome II or III. % Frequency of phenotype was quantified to the right and in panel g in reference to phenotypes observed in the R4 region. Dark green text/bars denote no activation of the reporter. Bright green text/bars denote a mild activation pattern. Purple text/bars bars denote the strongest activation pattern. 5–7 days old mated females were used for the experiment. (Right) Under homeostatic conditions, the reporter expresses GFP only in ISCs (dark green bar). At 6 hrs after 20HE feeding, GFP is localized in midgut progenitors all over the gut (bright green bar). 18% of the guts that express the reporter on chromosome II show a slight accumulation of GFP in other cells upon 20HE feeding, but the GFP signal was not as strong as in the category “GFP in many cells”.

(c-e) EcR is required in midgut progenitors (c) and enteroblasts (d) but not enterocytes (e) for transcriptional induction of *rho*, *upd2* *upd3* during the 2nd mitotic wave in response to 20HE feeding. In contrast, induction of *spitz* and *keren* are unchanged relative to 20HE fed controls. q-RT-PCR was performed on midguts from mated females 8 days after RNAi induction at 29°C followed by feeding with vehicle or 5mM 20HE for 16 hrs. Expression is indicated as mean fold change relative to vehicle-treated midguts \pm s.d. (n 3).

(f) ISCs need to proliferate in order for *rho*, *upd2* and *upd3* to be induced during the 2nd mitotic wave after 20HE feeding. *Egfr* and *Jak-Stat* signaling are transcriptionally induced 16 hrs post 20HE feeding. Control midguts have a transcriptional induction of *rho*, *upd2*, *Socs36E* and to a lesser extent *upd3* mRNA levels (vehicle denoted as purple versus control 20HE fed denoted as pink bars). Cell cycle arrest via string depletion or reduced *Egfr* signaling in midgut progenitors halts the upregulation of 20HE-induced *rho*, *upd2*, *Socs36E* and *upd3*. This data suggests that ISC division is cell autonomously controlled and this event is an initial requirement for the non-cell autonomous induction of promitotic factors to promote later ISC divisions. mRNA induction of *spitz* and *keren* is slightly decreased in string-depleted progenitors but are slightly higher in *Egfr* depleted progenitors relative to 20HE fed controls. Mated female midguts of wildtype flies, string or *Egfr* depleted progenitors for 8 days at 29°C were fed with vehicle or 5mM 20HE for 16 hrs then expression levels were determined by RT-qPCR. Expression is indicated as mean fold change relative to vehicle-treated midguts \pm s.d. (n 3).

(g) 20HE feeding induces activity of a *Jak-Stat* reporter more mildly than *P.e.* infection. Frequency of phenotype occurrence is analyzed based on the categories of activity in panel b. Under homeostatic conditions, the reporter expresses GFP only in ISCs (dark green bar). 16 hrs after 20HE feeding, most midguts of the reporter on chromosome II have GFP localized in many midgut cells including polyploid enterocytes (purple bar). However, most midguts of the reporter on chromosome III have GFP localized in the midgut progenitors (bright green bar). In contrast, *P.e.* infected midguts of the reporters on either chromosome showed a strong uniform activation pattern in all midgut cells of the R4 region. 5–7 days old mated females were used for the experiment.

(h) *upd3-lacZ* reporter is not activated by 20HE feeding. Images of the R4 region of the midgut showing basal expression of the *upd3* reporter in vehicle fed flies relative to strong

activation of the reporter upon *Pe.* infection. On the other hand, 16hrs of 20HE feeding did not appreciably activate the upd3 reporter. This data indicates that 20HE does not primarily activate upd3 to promote ISC mitoses in the midgut. 5–7 days old mated females were used for the experiment. All images were acquired at the same settings and the intensities of activation are accurately represented.

(i) (Left) Representative images of Erk activity, assayed as dpErk showing the most prevalent phenotype for each condition. (Right) Quantifications of the prevalence of each phenotype are shown. Under non-stressed conditions, dpErk is present either in very few ECs per gut, or in progenitor cells and very few ECs. Upon enteric infection, there is a strong upregulation of dpErk mainly in ECs. Although 20HE feeding also induces dpErk in midguts, the pattern is distinct from the one caused by enteric infection. Upon 20HE feeding, dpErk is mainly visible in progenitors and young ECs, and the signal is often localized to small patches of cells. In contrast, *Pe.* infection induces strong dpErk broadly throughout the gut. dpErk is absent in non-stressed upd2 or upd2,3 mutants. Enteric infection induces dpErk also in upd2 or upd2,3 mutants, albeit to a lower level than wildtype flies. In contrast, upd2 or upd2,3 mutants show very little or no dpErk upon 20HE feeding. 5–8 days old mated females were used for the experiment.

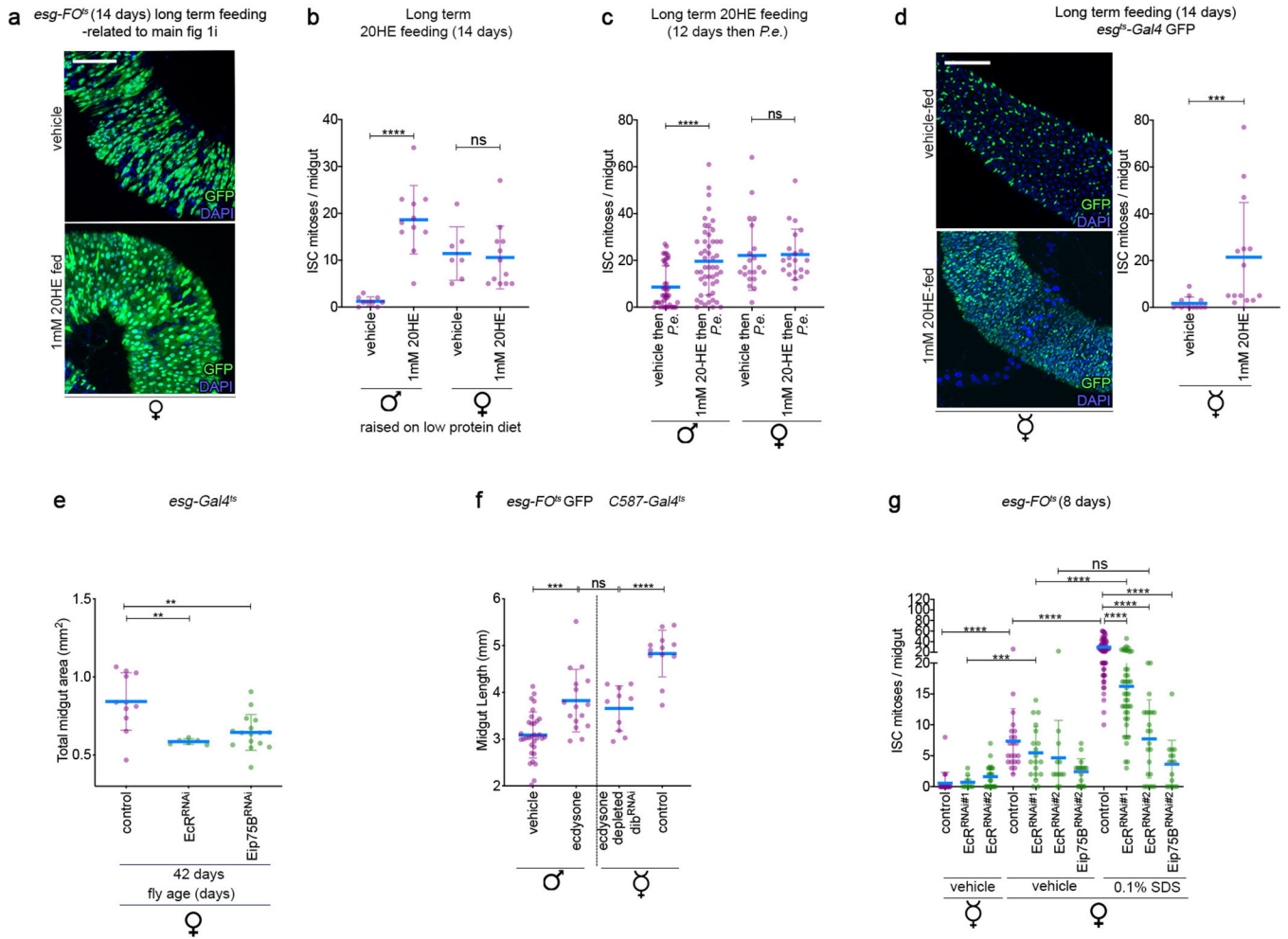
(j) Upd2, Egfr and rho are required in gut progenitors for the 2nd wave of mitoses induced by 20HE as shown by the diminished ISC mitoses 16 hrs after feeding 5mM 20HE to mated females with progenitor-specific depletion of Upd2, Upd2+Upd3, Egfr or rho.

(k) Upd2 and rho are required in enteroblasts for the 2nd wave of mitoses induced by 20HE as shown by the diminished ISC mitoses 16 hrs after feeding 5mM 20HE to mated females with EB-specific depletion of Upd2, Upd2 and Upd3 or rho. Results shown are for 2 different RNAi lines for Upd2.

(l) Upd2 but not Upd3 or rho is required in enterocytes for the 2nd wave of mitoses induced by 20HE as shown by the diminished ISC mitoses 16 hrs after feeding 5mM 20HE to mated females with enterocyte-specific depletion of Upd2, Upd2 and Upd3 or rho.

(m) Rho is partly required in EBs for the optimal ISC mitoses during the 1st mitotic wave in response to 6 hrs of 20HE feeding. ISCs were still able to divide at 6 hrs of 20HE feeding upon rho-depletion in EBs albeit at lower but non-significant levels relative to control flies. This result indicates that ISCs, with their intrinsic EGF signaling retain the ability to divide in response to 20HE in a cell-autonomous fashion.

For all panels, control flies express UAS-GFP instead of the transgene. The period of RNAi induction is indicated above every panel. Results in dot plots are from 3 independent biological replicates except for the qPCRs where the n numbers are indicated at the top of each panel. N = 10 are plotted for each genotype in the remaining scatter plots. Center is the mean and error bars represent \pm s.d. Statistical analyses were performed using Mann-Whitney test with two-tailed distribution. (ns = $P > 0.05$, * $P < 0.05$, ** $P < 0.01$, *** $P < 0.001$, **** $P < 0.0001$). Exact n numbers and P values > 0.0001 can be found in the online source data. Representative images are shown from experiments that were repeated 3–4 independent times. GFP, in green; DAPI, in blue. Scale bars = 100 μ m. The overnight standard period of feeding the flies was 16–20 hours. ♀ refers to mated females.



ED Fig. 4: Long-term 20HE feeding promotes sexually dimorphic ISC division and gut growth.

(a) 1mM 20HE feeding does not obviously increase epithelial turnover in females. Representative images are shown and are relevant to main Fig 1i.

(b) 20HE feeding causes male-specific midgut growth also on a low-protein diet, quantified by counting mitotic indexes of males and females raised on 20HE-laced low-yeast sucrose solution or sucrose-yeast solution as vehicle. 20HE- or vehicle-fed female ISCs did not differ in their mitotic counts. However, 20HE-fed males had a strong increase in their mitotic index compared to vehicle-fed males.

(c) 20HE feeding enhances ISC mitotic activity in *Pe* infected males, altering their behavior to resemble *Pe*-induced ISC division in females, assayed by mitotic counts of males and females. Flies were raised on 20HE or vehicle-supplemented food for 12 days then the treatment was withdrawn overnight followed by *Pe* infection for 20 hrs. Male ISCs that were 20HE-fed were able to respond to *Pe* infection at similar rates to the age-controlled females fed on 20HE or vehicle.

(d) 20HE-fed virgins undergo epithelial turnover much faster than age-controlled virgins, which have infrequently dividing ISCs. (Left) Representative images and (Right) quantification of mitotic counts from control virgin flies 14 days after +/-20HE feeding.

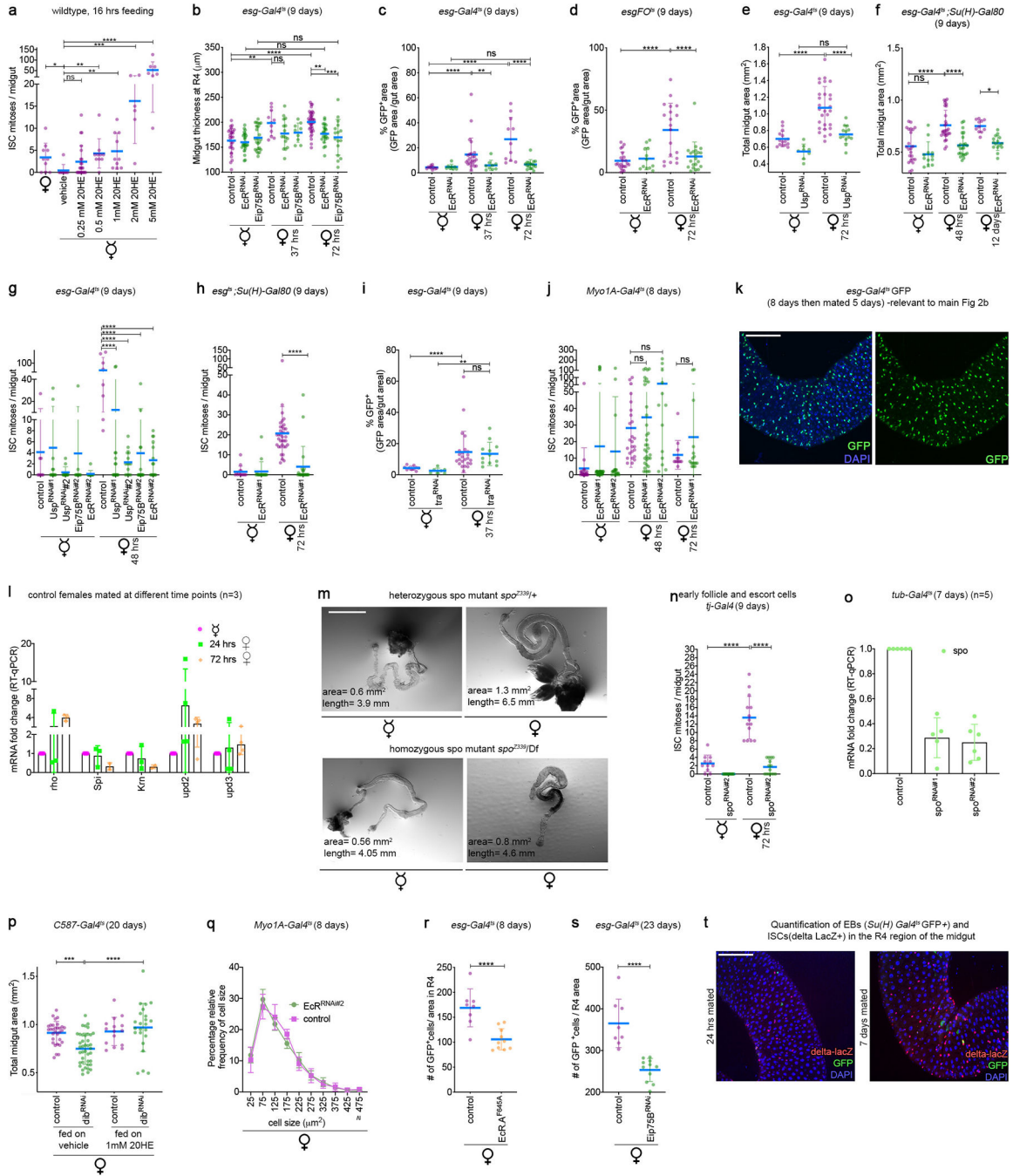
Both the frequency of dividing ISCs and progenitor cells of 20HE fed virgins resemble the behavior of mated females.

(e) Eip75 and EcR are required in midgut progenitors to maintain proper midgut size, quantified as midgut areas in images of guts from mated females with progenitor-specific depletion of EcR or Eip75B aged for 42 days.

(f) Quantification of midgut lengths of control males, 20HE-fed males, control virgin females, or virgin females depleted of ecdysone via ovary-specific knockdown of *dib^{RNAi}*, shows the plasticity of male and female midgut growth to 20HE levels. 20HE-fed males have increased midgut length in contrast to *dib^{RNAi}* female virgins, with decreased 20HE levels and strikingly shorter guts. In both cases there was a one third gain or loss in midgut length in comparison to a control male or virgin female respectively.

(g) Ecdysone signaling via EcR and Eip75B is required in ISC clones of mated females for maximal proliferation in response to SDS. ISC mitotic counts of virgin females are minimal under basal conditions. Upon SDS feeding, control ISC clones divide to regenerate the epithelium but EcR or Eip75B depleted ISC clones are significantly impaired in their ability to divide. RNAi was induced in ISC clones for 8 days before 16–18 hrs of 0.1% SDS feeding.

For all panels, control flies express UAS-GFP instead of the transgene. The period of RNAi induction is indicated above every panel. Results in dot plots are from 3 independent biological replicates. N = 10 are plotted for each genotype in the remaining scatter plots. Center is the mean and error bars represent \pm s.d. Statistical analyses were performed using Mann-Whitney test with two-tailed distribution, except panel f: ordinary ANOVA test, followed by Bonferroni's multiple comparisons test (ns $P > 0.05$, ** $P < 0.01$, *** $P < 0.001$, **** $P < 0.0001$). Exact n numbers and P values > 0.0001 can be found in the online source data. Long term 20HE feeding indicates that 1mM 20HE was fed to the flies for 12 days or 14 days in panels c and a,b,d consecutively. Representative images are shown from experiments that were repeated 3 independent times. GFP, in green; DAPI, in blue. Scale bars = 100 μ m. σ refers to males, \varnothing refers to virgins and φ refers to mated females.



ED Fig. 5: Mating requires ecdysteroidogenic enzymes from the early ovarian follicles and escort cells to induce ISC divisions in the gut through EcR/Usp which causes increased stem cell number and subsequent gut growth.

(a) 20HE induces ISC mitoses in a dose-dependent manner in ISCs of virgin females. Virgin females were fed with different doses of 20HE and their mitotic indexes were assessed after 16–18hrs of feeding. At 0.25–1mM 20HE, ISCs divide similar to basal levels in mated females. At 2mM 20HE feeding, ISCs mildly divide (3–4× higher than divisions induced by 1mM 20HE). At 5mM 20HE, ISCs divide at 10–11× higher than divisions induced by 1mM 20HE.

- (b)** The increase in width of the R4 region in response to mating in females requires EcR and Eip75B in progenitors.
- (c)** EcR is required in intestinal progenitors for their accumulation upon mating, shown by quantification of the GFP⁺ labeled areas of progenitors in the midgut upon progenitor-specific depletion of EcR \pm mating at early and later time points after mating.
- (d)** EcR-depleted ISC clones are unable to divide in response to mating, as quantified by GFP⁺ clonal area in EcR-depleted ISC-derived clones and age-matched control clones. ISC-derived clones in control females have GFP⁺-labeled ISCs and all their subsequent progeny stably express GFP as well.
- (e)** Usp is required in progenitors for the mating-induced midgut growth as shown by quantification of midgut areas in females with Usp-depleted progenitors \pm mating.
- (f)** EcR is cell-autonomously required in ISCs for mating-induced midgut growth, shown by quantification of midgut areas in females with EcR-depleted ISCs \pm mating. After the first mating, control female midgut initially grows and midgut growth persists in flies that are raised repeatedly mated. This midgut growth requires EcR functions in ISCs.
- (g)** Ecdysone signaling via EcR, Usp and Eip75B are required in midgut progenitors for the mating-induced mitotic response, as shown by the reduced ISC mitoses upon 48hrs mating in female midguts with progenitor-specific depletion of EcR, Usp or Eip75B. Virgins were left to mate for 48hrs prior to dissection, then mitotic counts were assessed. Results shown are for a 2nd RNAi line to complement the results in Fig 2.
- (h)** EcR is cell-autonomously required in ISCs for mating-induced ISC mitoses shown by mitotic counts of midgut in females with EcR-depleted ISCs 72hrs after mating. These results are done with a 2nd independent RNAi to complement main Fig 2f.
- (i)** Masculinized *tra*^{RNAi} progenitors undergo mating-induced expansion of GFP⁺ progenitors similar to controls, indicating that the mating effects on progenitors are independent of the sex determination pathway, quantified as GFP⁺ area of progenitors in the R4 region. Virgins typically have GFP-marked single cells (ISCs) or few pairs (ISC-EB). Shortly after mating, the ISC cells divide and the resulting progeny are transiently marked with GFP, but then turn off GFP expression as they differentiate.
- (j)** EcR is not required in ECs for mating-induced ISC mitoses. 48 hrs to 72 hrs after mating, ISCs of EcR depleted ECs midguts divide at similar rates to control midguts indicating that EcR in ECs is dispensable to mating-induced ISC mitoses. Results shown are for 2 different RNAi lines.
- (k)** Representative confocal image of GFP expressing progenitors using *esg^{GS}* in females 5 days post mating. Flies were raised as virgins and were aged 8 days similar to conditions in main Fig 2b then mated for 5 days. Females were always mated to males with no genetic manipulations. Equal number of males and females were allowed to mate (a ratio of 1:1). Image is acquired in the R4 region. This suggests that the strong mitotic effect of mating is transient. GFP, in green; DAPI, in blue. Scale bar, 100 μ m.
- (l)** *Rho* and *upd2* are transcriptionally upregulated in female midguts 24 hrs (green symbols) or 72 hrs (orange symbols) after mating relative to virgins (pink symbols). 5–7 days old control virgins were mated for 24 or 72 hrs then mRNA expression levels were determined by RT-qPCR. Expression is indicated as mean fold change relative to vehicle-treated midguts \pm SD (n=4).

(m) Representative images of whole body *spo* mutants that are either heterozygous and hence viable with no growth or egg laying defects (upper panels) or sterile, homozygous *spo* mutants rescued to adulthood with by a pulse of 20HE given to dechorionated embryos (lower panels). Images are complementary to main Fig 2i. Scale bar 1mm.

(n) RNAi-mediated depletion of *spo* in ovaries blunts ISC mitoses in response to mating. The traffic jam (*tj-Gal4*) driver that is expressed in somatic gonadal cells was used for *spo* depletion. Flies were raised as virgins then mated for 72hrs.

(o) *spo* RNAi depletes the *spo* gene efficiently. Constitutive driver *tub⁶⁵* was used to deplete *spo* in mated females for 8 days then mRNA expression levels were determined by RT-qPCR. Expression is indicated as mean fold change relative to vehicle-treated midguts \pm s.d. (n=4).

(p) Ovary-derived ecdysone is required for the proper size of the midgut, shown by quantification of midgut areas in mated female midguts depleted of 20HE-synthesizing enzyme *dib* in the ovary. *C587ts* driver, which is expressed in escort cells and immature follicle cells of the ovary, is used to induce ecdysteroidogenic enzymes depletion. Decreased midgut area in mated females with reduced 20HE levels is completely rescued by raising females on exogenous 1mM 20HE. *Dib* RNAi was validated in ³⁷ and other reports.

(q) Depletion of EcR in midgut enterocytes does not significantly decrease their size 8 days after mating. Cells of the midgut were stained with CellMask, a plasma membrane stain, and a custom macro (Supplementary Data 1) was used to segment the cells according to size. Shown is a frequency distribution of the different cell sizes. EcR depleted enterocytes have a bigger proportion of cells sized 75–175 μm^2 than control midguts. However, the differences in distribution of the cell sizes are statistically non-significant. Data are from n 5 stacks of midguts taken at the R4 region.

(r) Basal levels of EcR signaling are required to maintaining the optimal number of progenitors in the midgut as shown by quantification of GFP+ progenitors in mated females expressing EcR A DN in comparison to the control.

(s) Basal levels of Eip75B are required for maintenance of ISCs in non-stressed flies, quantified by the number of GFP+ progenitors in mated females after progenitors-specific depletion of Eip75B. A small reduction of progenitor numbers (~25%) implies that Eip75B is not critically required for ISC survival. Note that y-axis does not go to zero.

(t) Control midguts display an increase of delta+ cells at several time points following mating shown by quantification of delta+ (red) and Su(H)+ (green) cells. At 24 hrs post mating, most delta+ cells remain singlets, similar to virgins. At 40 hrs post mating, most delta+ cells expand to become doublets to triplets (main Fig 2k). At 7 days after the 1st mating most delta positive cells are again singlets, however their numbers are irreversibly increased relative to virgins. Females were mated to males with no genetic manipulations. Equal number of males and females were allowed to mate (a ratio of 1:1) and females were allowed to mate for 18–20 hrs after which males were removed, except for the condition “raised mated for 7 days” whereby males were always in the vial with the females. Images are acquired in the R4 region. This suggests that mating induces an initial symmetric increase in the number of ISCs that is irreversible. Representative images for other conditions and quantifications are shown in main Fig 2k. Each dot represents a gut, and % of delta+ or Su(H)+ cells are calculated from absolute number of positive cells relative to total DAPI+ cells. delta, in red; GFP, in green; DAPI, in blue. Scale bar, 100 μm .

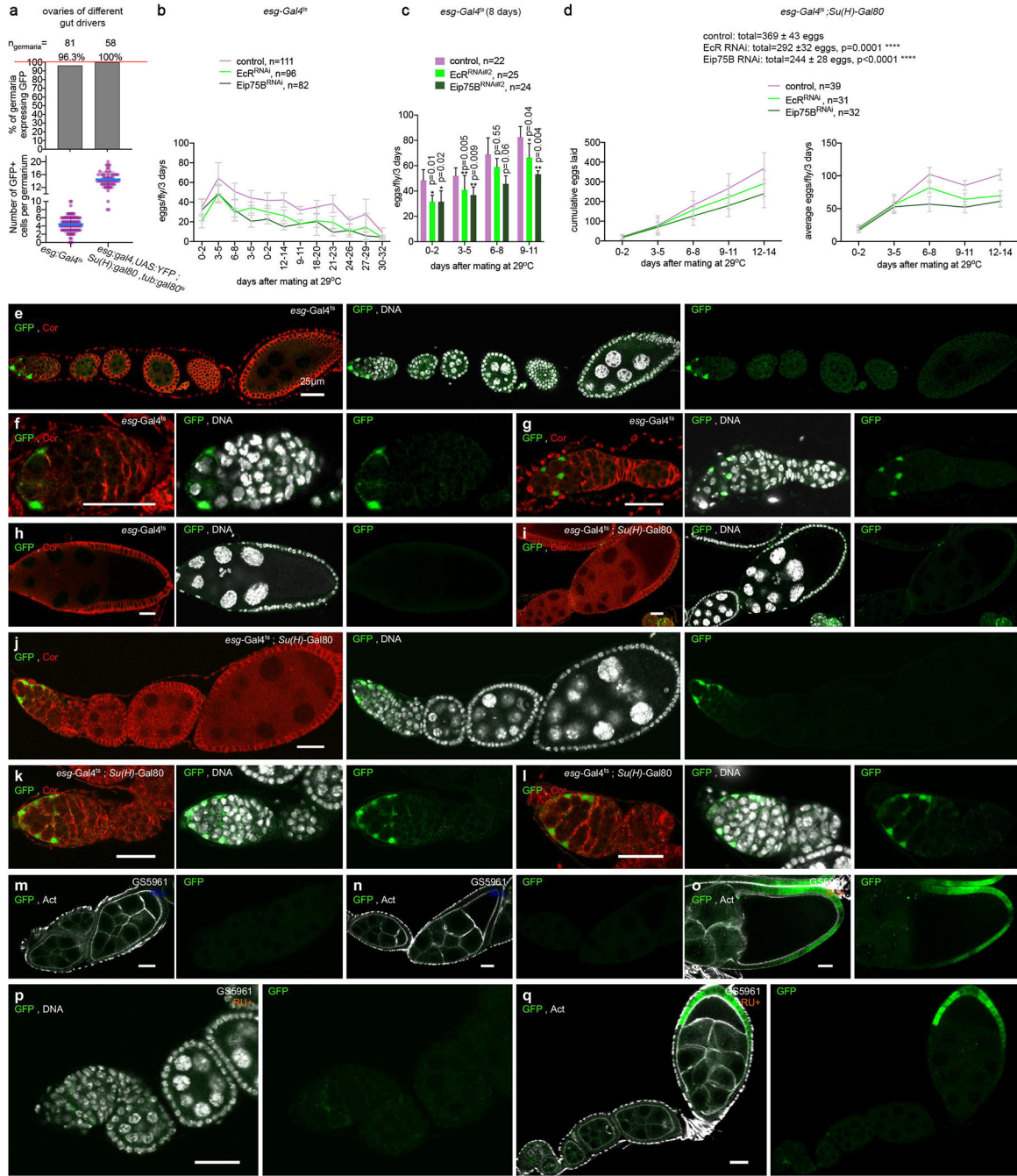
For all panels, control flies express UAS-GFP instead of the transgene. The period of RNAi induction is indicated above every panel. Results in dot plots are from 3 independent biological replicates. N = 10 are plotted for each genotype in the remaining scatter plots. Center is the mean and error bars represent \pm s.d. Statistical analyses were performed using Mann-Whitney test with two-tailed distribution, except for gut measurements in panel b,e,f,p: ordinary ANOVA test, followed by Bonferroni's multiple comparisons test (ns = $P > 0.05$, * $P < 0.05$, ** $P < 0.01$, *** $P < 0.001$, **** $P < 0.0001$). Exact n numbers and P values > 0.0001 can be found in the online source data. Representative images are shown from experiments that were repeated 3 independent times. ♂ refers to virgins and ♀ refers to mated females.

Author Manuscript

Author Manuscript

Author Manuscript

Author Manuscript



ED Fig. 6: Ovaries of the *esg-Gal4^{TS}, esg^{TS} Su(H)-Gal80* midgut drivers have GFP expression in their germaria in a subset of escort cells.

(a) (top graph) Most midgut drivers express GFP in ovary germaria. The frequency of germaria expressing GFP is displayed in the bar graph. Ovaries of the *esg^{TS}* driver have some escapers that have no GFP in their germarium while almost all ovaries of the *esg^{TS} Su(H)gal80* driver have no escapers and all ovaries express GFP. (bottom graph) Number of GFP+ cells per germarium for both midgut drivers *esg^{TS}* or *esg^{TS} Su(H)gal80*, which are expressed in midgut progenitors and ISCs respectively. Further examination of *esg^{TS}* driver shows that it is expressed in ~4 escort cells while *esg^{TS} Su(H)gal80* driver shows expression

in ~14 escort cells. Number of germaria analyzed is indicated above each driver. Control germaria typically have 45–70 escort cells³⁸.

(b) Mated females with EcR or Eip75B depleted midguts have reduced reproductive output. This graph is related to the experiment presented in Fig 2p. Average eggs/fly/3 days are plotted instead of the cumulative sums. Flies that died during the experiment were excluded in the analysis.

(c) Mated females with EcR or Eip75B depleted midguts have reduced reproductive output. Flies with control, EcR- or Eip75B-depleted midgut progenitors were raised as virgins for 8 days then were allowed to mate to males with no genetic manipulations at a ratio of 1:1 in populations of 5 females and 5 males. Eggs were collected from the fly vials every day for up to 11 days and the average total eggs/fly every 3 days is plotted. An independent alternative 2nd RNAi is shown to complement data in main Fig 2p. Means are shown with error bars representing s.d. and p-values are calculated by t-test with two-tailed distribution assuming unequal variance.

(d) Mated females with EcR or Eip75B depleted ISCs have reduced reproductive output. Flies with control, EcR- or Eip75B-depleted midgut ISCs were raised at 18°C for 2 days maximum then were shifted to 29°C and allowed to mate to males with no genetic manipulations at a ratio of 1:1. Flies were pooled together the first night of mating to ensure mating then on the next day, single females were housed with a control male in single vials. Eggs were collected from the fly vials every 48 hrs for up to 14 days. Flies that died during the experiment were excluded in the analysis. (Left) graph shows the cumulative eggs laid across 14 days \pm s.d.. (Right) graph shows the average total eggs/fly every 3 days plotted across 14 days \pm c.i. *P*-values were calculated by *t*-test with two-tailed distribution assuming unequal variance. Exact *n* numbers for a-d can be found in the online source data.

(e-h) *esg-Gal4^{ts}* and the *esg^{ts} Su(H)-Gal80* drive expression in a small number of ovary escort cells. *Drosophila* ovaries are composed of 16 ovarioles. At the anterior tip of every ovariole the germarium contains the germline stem cells and the somatic stem cells which constantly produce follicles or egg chambers. As the follicles progress to the posterior end of the ovariole they develop to lead to the formation of a mature egg. Follicle development is divided into 14 stages. In the most anterior part of the germarium (Region I) the cap cells and the escort cells constitute the niche required for the maintenance of the GSCs and the proper differentiation of the early germline cyst. We detected expression of the *esg-Gal4^{ts}* and the *esg^{ts} Su(H)-Gal80* drivers within the germarium in a subset of escort cells (a). Confocal sections of follicles from stage 2–7 (e), stage 9 (h) and germaria (f,g) isolated from *esg-Gal4^{ts}* flies and stained for GFP (green), Coracle (red) and DNA (DAPI, gray). No GFP signal was detected in follicles from stage 2 to 9 (e,h) or in later stages (not shown). However, 96% of germaria showed GFP in a subset of cells in the anterior region I (f,g). The GFP expressing cells were located in between the germline cysts and exhibited a triangular shape indicating that they were the escort cells.

(i-l) All germaria from *esg^{ts}Su(H)-Gal80, UAS-GFP* flies express GFP in escort cells (a,j,k,l) and no GFP expression was detected from stage 2 to 9 (i,j) or in later stages (not shown).

(m-q) We detected expression of the Switch GS5961-Gal4 driver within ovaries in the posterior follicular cells from stage 8 of oogenesis. Confocal section of follicles isolated from GS5961/UAS-GFP flies kept 4 days on yeast paste only (RU-) or yeast paste

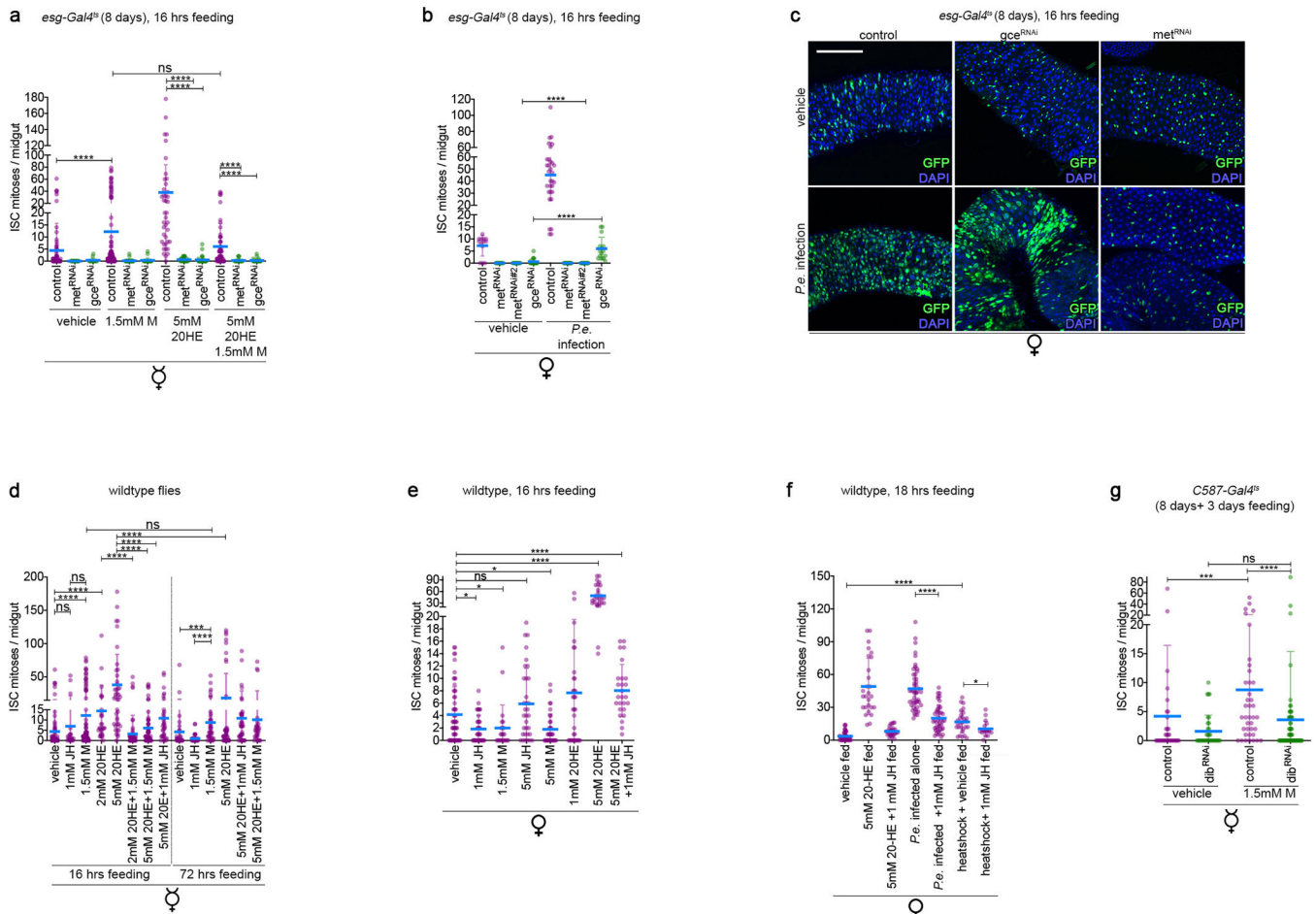
supplemented with RU486 (RU+) for 4 days and stained for GFP (green), actin (phalloidin, gray) or DNA (DAPI, gray). In absence of RU induction no GFP was detected in the ovary (m,n). After RU feeding no expression was detected in germaria or follicles prior to stage 7 (p,q). At stage 7 a subset of the most posterior follicular cells started to express weakly the GFP, this expression was then stronger and spreading to more follicular cells in a posterior to anterior gradient during stage 8 of oogenesis (q - most posterior follicle) and maintained later on in most of the posterior follicular cells that cover the oocyte (o - stage10). All pictures are presented with the anterior on the left and the posterior on the right.

Author Manuscript

Author Manuscript

Author Manuscript

Author Manuscript



ED Fig. 7: JH receptors are required for ISC divisions while exogenously fed JH inhibits ISC mitoses in response to other promitotic stimuli.

(a) JH receptors *met* and *gce* are required for exogenously fed 20HE to induce ISC mitosis. Virgin females were fed with 1.5mM methoprene, 5mM 20HE, or 20HE and methoprene in combination, and their mitotic indexes were assessed after 16–18hrs of feeding. Knockdown of *met* or *gce* in progenitors blunted the proliferative response to all three fed stimuli. Virgins were aged for 8 days at permissive temperature then fed with the different hormone regimes for 16–18 hrs.

(b-c) *met* and *gce* receptors are required in midgut progenitors of mated females for *Pe.*-induced ISC mitoses. Mated females of indicated genotypes were aged for 8 days at permissive temperature then fed with *Pe.* for 18–20hrs. ISC mitotic counts are shown in (b). Images of progenitor accumulation after *Pe.* feeding to mated females are in (c).

(d) Methoprene induces ISC mitoses in ISCs of virgin females. Virgin females were fed with active JH III ligand (“JH”), JH agonist methoprene (“M”), 2mM or 5mM 20HE, or two compounds in combination, and their mitotic indexes were assessed after feeding for 16–18 hrs (left side) or 72hrs (right side). After 16–18 hrs of feeding, the average number of ISC mitoses per midgut were as follows. vehicle fed: 3.8, 1mM JH: 6.6, 1.5mM methoprene: 8, 2mM 20HE: 14, 5mM 20HE: 41. A combination feeding of 1.5mM methoprene with either 2mM 20HE or 5mM 20HE blunts mean ISC mitoses to 3.6 or 2.3 respectively. Combination

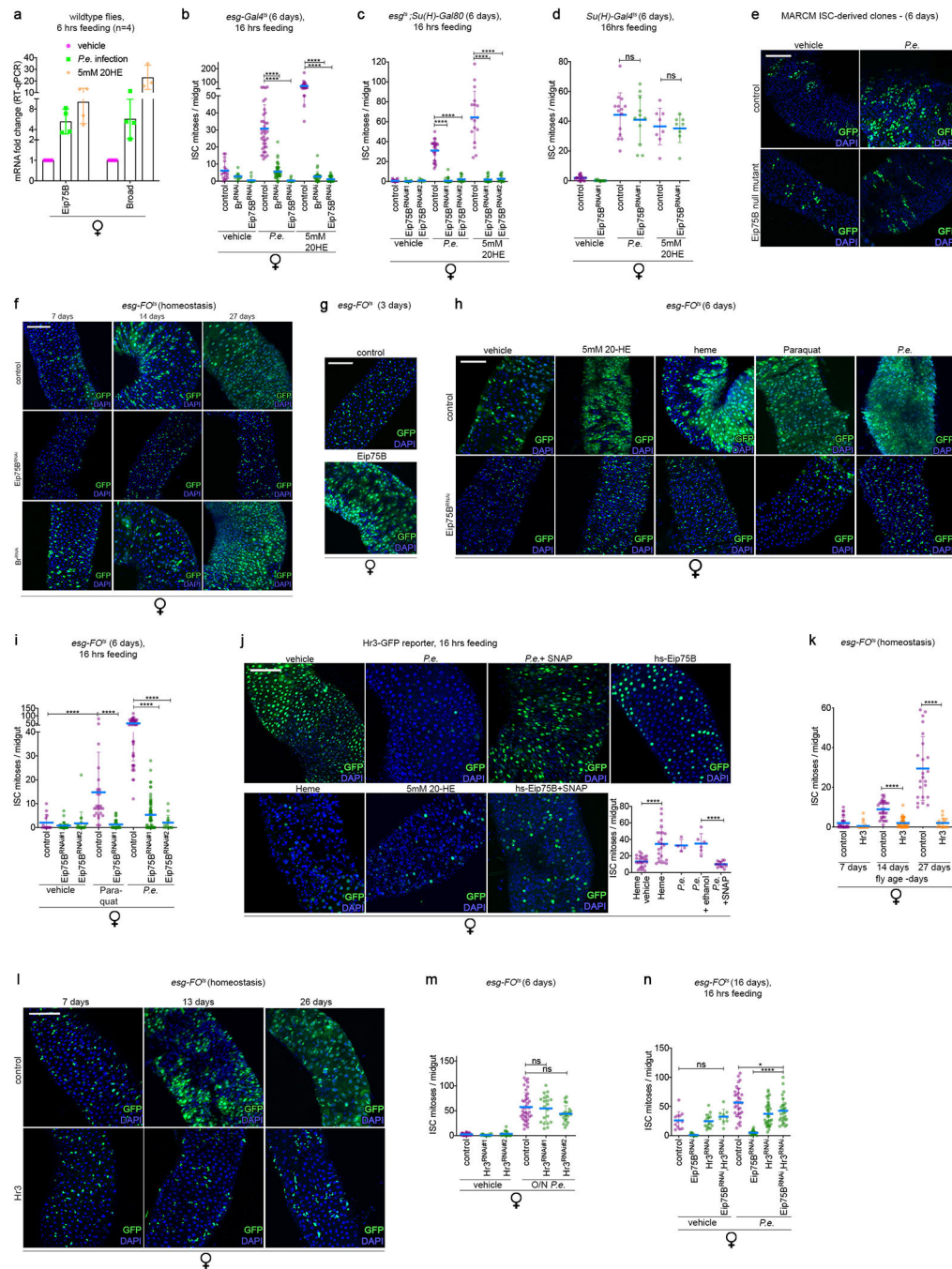
feeding of 1mM JH with 5mM 20HE suppresses mean ISC mitoses to 11.5. After 72 hrs of feeding, the average number of ISC mitoses per midgut were as follows. Vehicle control: 5.5, 1.5mM methoprene: 9.5, 5mM 20HE: 13.5 mitoses, 5mM 20HE + 1mM JH 10.9, 5mM 20HE + 1.5mM methoprene: 10. These results indicate that 16 hrs of 2–5mM 20HE act as a strong promitotic signal to ISCs of virgin females, but after 72hrs the mean 20HE-induced mitoses drop towards basal levels. 1.5mM methoprene causes a mild but persistent increase in ISC mitoses over 72 hrs. Overnight combination feeding of 20HE and 1.5mM methoprene or 1mM JH strongly suppressed 20HE-induced mitoses.

(e) Methoprene does not promote ISC mitoses in mated females. Mated females were fed with 1mM or 5mM active JH III ligand (“JH”), JH agonist methoprene (“M”), 1mM or 5mM 20HE, or 20HE and JH in combination and their mitotic indexes were assessed 16–18 hrs after feeding. Feeding of 1mM or 5mM JH, 1mM 20HE, 1.5mM or 5mM methoprene do not induce mitoses in mated females. 5mM 20HE feeding induces a boost of ISC mitoses that were suppressed by combination feeding with 1mM JH.

(f) Exogenous JH feeding inhibits ISC mitoses when combined with other promitotic stimuli. Mated females were heat-shocked for 30 mins, infected with *Pe.* for 18–20 hrs or fed with 20HE, either alone or in combination with 1mM JH feeding for 16–18hrs, and mitotic indexes were scored. In each case, feeding 1mM JH suppresses the mitotic response of the stimulus.

(g) Ovarian ecdysteroidogenic enzymes are required for methoprene-induced mitoses of the midgut. 1.5mM methoprene causes ISC mitoses in control midguts (mean of 6.5 mitoses relative to 2 mitoses in vehicle-fed flies). In animals where the ecdysteroidogenic enzyme *dib* is depleted in ovaries, methoprene failed to significantly induce ISC proliferation (mean of 3.3 mitoses relative to mean of 1.4 basal mitoses in *dib*^{RNAi} vehicle-fed flies). Virgins were aged for 8 days at permissive temperature then fed with the different hormone regimes for 3 days.

For all panels, control flies express UAS-GFP instead of the transgene. The period of RNAi induction is indicated above every panel. Results in dot plots are from 3 independent biological replicates. N = 10 are plotted for each genotype in the remaining scatter plots. Center is the mean and error bars represent \pm s.d. Statistical analyses were performed using Mann-Whitney test with two-tailed distribution (ns: $P > 0.05$, * $P < 0.05$, ** $P < 0.01$, *** $P < 0.001$, **** $P < 0.0001$) Exact *n* numbers and *P* values > 0.0001 can be found in the online source data. Representative images are shown from experiments that were repeated 3 independent times. ♀ refers to virgins and ♂ refers to mated females.



ED Fig. 8: Eip75B is a downstream ecdysone-inducible effector required to stimulate ISC proliferation, through Hr3 repression.

(a) 20HE feeding or *Pe* infection transcriptionally upregulate the ecdysone-inducible targets Eip75B and broad. 5–7 day old mated females were fed with 20HE or infected with *Pe* for 6 hrs, then mRNA levels were determined by RT-qPCR on RNA from whole midguts. Expression is indicated as mean fold change relative to vehicle-treated midguts ± s.d. (n=4).

(b) Broad and Eip75B are required by adult *Drosophila* midgut progenitors for *Pe* or 20HE-induced ISC mitoses. Increased mitoses were observed upon *Pe* infection or 20HE-

in control mated flies, which were significantly blunted upon Broad or Eip75B depletion in midgut progenitors.

(c-d) Eip75B is only cell-autonomously required in ISCs (c), but not EBs (d) for *Pe.*- or 20HE-induced ISC mitoses. Flies were fed with 20HE or *Pe.* for 16–20 hrs. Results are shown for 2 independent RNAi lines.

(e) Eip75B null mutant clones are strongly impaired in their ability to divide and regenerate the epithelium. Eip75B null mutant clones were generated by MARCM and analyzed 6 days after *Pe.* infection. This experiment was done with a different recombinant mutant stock than the one used in ED Fig 2.

(f) *Eip75B^{RNAi}* blocks midgut epithelial renewal; *Broad^{RNAi}* does not. Representative images from ISC clones of aging epithelia with reduced levels of Eip75B or Broad. Broad depletion does not affect ISC clonal growth while Eip75B depletion blocks any ISC growth and most cells remain singlets.

(g) Eip75B overexpression in ISC-derived *esgFO^s* clones is pro-proliferative as shown by representative images of ISC clones in the epithelium of mated females.

(h-i) Eip75B is required by ISCs to divide in response to 20HE, heme, Paraquat and enteric infection. (h) Representative images of Eip75B-depleted ISC clones in response to the different stresses. Clonal growth to any stress stimulus is impaired. (i) Quantification of mitotic counts is shown. Results for *Pe.*-induced mitoses are shown for 2 independent Eip75B RNAi lines.

(j) Representative images of the heatshock inducible Hr3 reporter (*hs-Gal4.DBD-Hr3.LBD>GFP*) are shown. Conditions of low Eip75B activity result in high Hr3 reporter expression and high Eip75B activity is reflected by low Hr3 reporter expression. Of note, owing to its transcriptional repressive activity, Eip75B reporter cannot be used to monitor its activity³². Under basal conditions, midguts express high levels of Hr3 reporter. Hr3 activity is repressed by 20HE or heme feeding, *Pe.* infection (stimuli that require Eip75B) or co-expression of *Eip75B*. Nitric oxide (NO) inhibits Eip75B binding to Hr3³⁹. SNAP is a NO donor compound that modulates NO availability and is used to regulate Eip75B activity. However, increased NO levels through SNAP feeding relieved *Pe.* and *Eip75B*-repressive actions on GFP expression. This indicates that in ISCs Eip75B inhibits Hr3 while NO blocks this suppressive effect. (Right) Mitotic counts are shown for vehicle-fed, heme-fed, *Pe.*, or *Pe.*+SNAP-fed mated females after 30 mins heatshock (to induce the Hr3-GFP reporter) and 18–20 hrs of feeding.

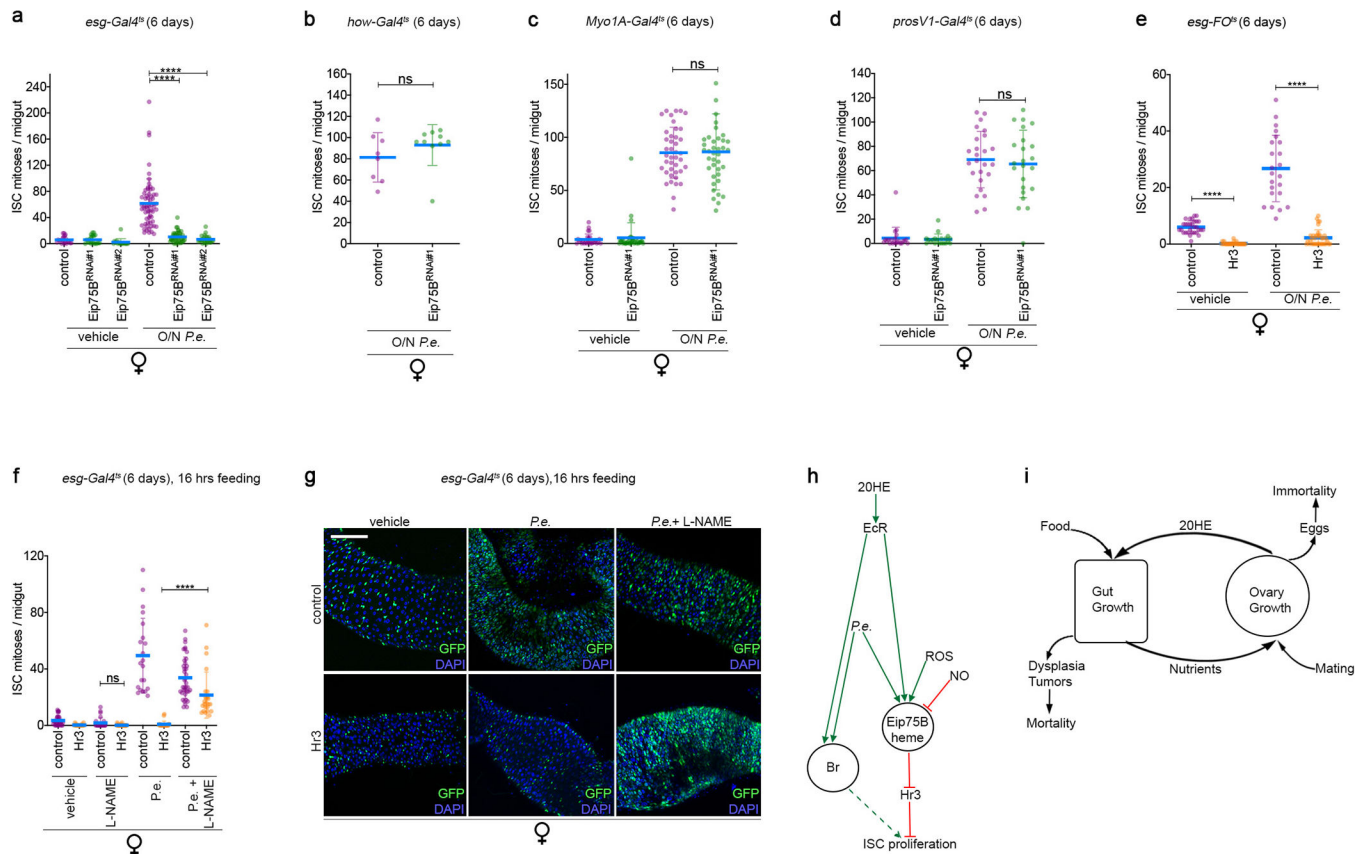
(k-l) Hr3 overexpression strongly impairs epithelial renewal as the flies age, depicted by quantifications of mitotic indexes in (k). Representative images of GFP-marked Hr3-overexpressing ISC clones showing impaired clonal growth in midguts of mated females (l).

(m) Hr3-depletion permits ISCs to divide in response to *Pe.* infection as shown by mitotic counts of Hr3-depleted ISC clones in mated females, which respond to *Pe.* infection at similar rates as control midguts.

(n) Repression of ISC mitoses in Eip75B-depleted *esgFO^s* clones is rescued by *Hr3^{RNAi}* as shown by mitotic counts of aging or *Pe.*-infected guts with Eip75B, Hr3 depletion or both. This experiment shows that Hr3 is epistatic to Eip75B.

For all panels, control flies express UAS-GFP instead of the transgene. The period of RNAi induction is indicated above every panel. The overnight standard period of feeding the flies was 18–20 hours. Results in dot plots are from 3 independent biological replicates. N 10 are

plotted for each genotype in the scatter plots. Center is the mean and error bars represent \pm s.d. Statistical analyses were performed using Mann-Whitney test with two-tailed distribution (ns: $P > 0.05$, **** $P < 0.0001$). Exact n numbers and P values > 0.0001 can be found in the online source data. Representative images are shown from experiments that were repeated 3 independent times. GFP, in green; DAPI, in blue. Scale bars = 100 μm . ♀ refers to mated females.



ED Fig. 9: NO modulates the interaction of Eip75B and Hr3 to regulate ISC division.

(a-d) Eip75B is not required in other midgut cell types besides progenitors for *Pe.* infection to induce ISC proliferation. Eip75B was depleted in (a) progenitors using *esg-gal4^{ts}* (2 independent RNAi lines are shown to complement results in main Fig 2), (b) visceral muscle using *how-Gal4^{ts}*, (c) enterocytes using *Myo1A-gal4^{ts}*, or (d) enteroendocrine cells using *prosV1-gal4^{ts}*.

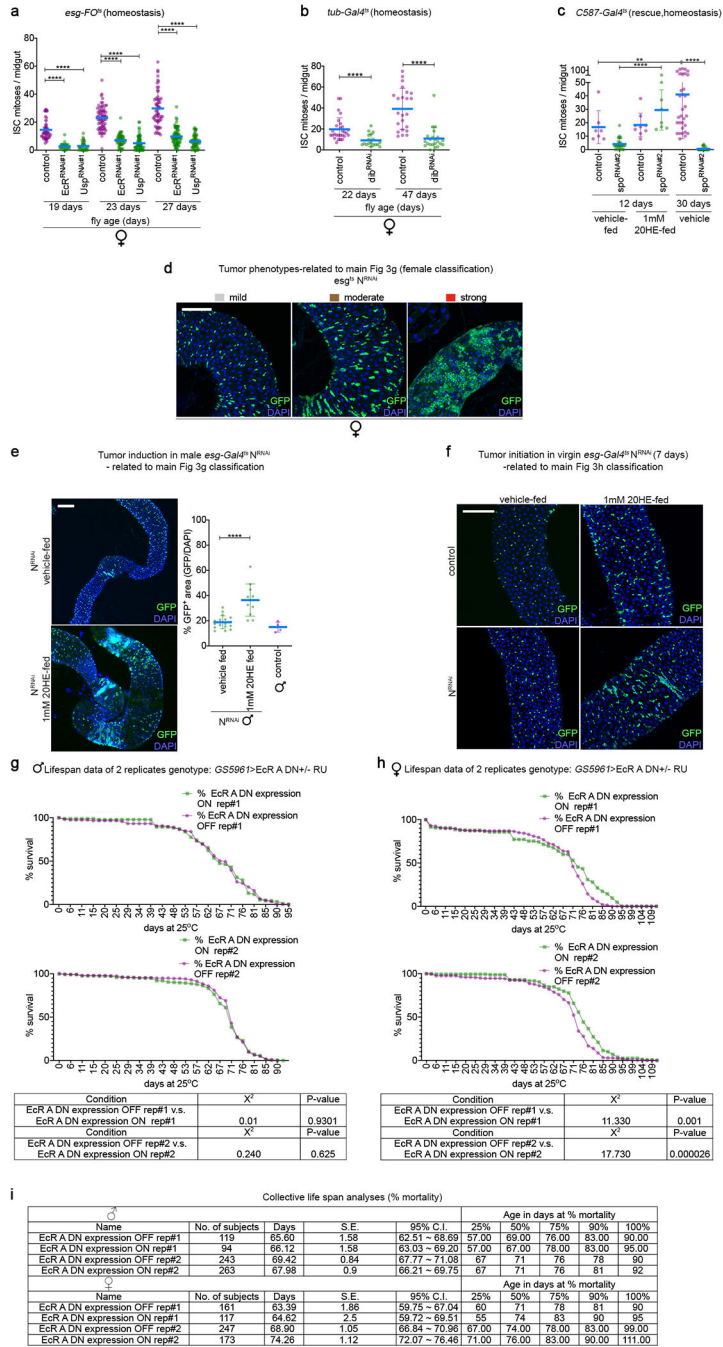
(e) Overexpression of Hr3 in ISC-derived clones impedes the mitotic ability of ISCs to divide in response to *Pe.* infection.

(f-g) NO inhibition rescues the ISC mitotic activity of Hr3-overexpressing progenitors. (f) ISC mitotic counts. (g) Representative images of progenitor-specific overexpression of GFP +/- Hr3 followed by *Pe.* infection alone or in combination with L-NAME, an NO inhibitor. NO represses the ability of Eip75B to interact with Hr3 hence, allowing transcriptional regulation of Hr3 targets. Treatment with L-NAME rescued the ISC ability to divide and progenitors expanded to fill the epithelium similar to the control mated females after infection. (compare to results in ED Fig 8j).

(h) Model summarizing the regulation of Eip75B, Hr3 and broad.

For all panels, control flies express UAS-GFP instead of the transgene. The period of RNAi induction is indicated above every panel. The overnight standard period of feeding the flies was 18–20 hours. Results in dot plots are from 3 independent biological replicates. N = 10 are plotted for each genotype in the scatter plots. Center is the mean and error bars represent ± s.d. Statistical analyses were performed using Mann-Whitney test with two-tailed

distribution (ns: $P > 0.05$, **** $P < 0.0001$). Exact n numbers and P values > 0.0001 can be found in the online source data. Representative images are shown from experiments that were repeated 3 independent times. GFP, in green; DAPI, in blue. Scale bars = 100 μm . ♀ refers to mated females.



ED Fig. 10: Ovary-derived 20HE promotes intestinal dysplasia through EcR, Usp and Eip75B, which may affect *Drosophila* life span.

(a) The number of mitotic cells in midguts increases with age, and this is inhibited by RNAi mediated knockdown of EcR or Usp in ISC clones (*esgFO^{Δ5}*). Mitotic counts are shown at 19, 23, and 27 days post-eclosion in non-stressed female guts.

(b) Basal 20HE levels promote age-dependent intestinal dysplasia. Mitotic indexes are shown in aged mated female midguts from flies ubiquitously expressing *dib^{RNAi}* at 2 different ages after RNAi induction.

(c) Ovary ecdysone is required for ISC mitoses in non-stressed animals. Young and old mated females with *spo* knockdown in their ovaries have reduced ISC mitoses compared to controls. This was rescued by feeding the flies 1mM 20HE. A 2nd independent RNAi for *spo* is shown to complement data in main Fig 2.

(d) Representative images for the three classes of tumor phenotypes used to score mated female tumors in main Fig 3.

(e) 20HE feeding potentiates the tumor growth in *N^{RNAi}* males. (Left) Representative images with which males have been scored in main Fig 3. Males exhibiting big tumor clusters of at least 30 neighboring cells along the gut were classified strong. In contrast, guts with one or 2 tumor clusters with less than 10 neighboring cells were classified mild. (Right) Quantifications are derived by calculating the ratio between GFP+ area / DAPI+ area. Tumor induction was commenced a few days prior to 20HE feeding.

(f) 20HE feeding potentiates the tumor initiation in virgin females with *N^{RNAi}*. Representative images are shown for the quantifications presented in main Fig 3. Guts with no tumor clusters and just doublets of progenitor cells were classified mild. Guts with tumor clusters of less than 10 neighboring cells were classified moderate and guts with tumor clusters of at least 30 neighboring cells were classified strong.

(g-i) Progeny of the genotype *GS5961-Gal4 UAS-EcR^{F645A}* were mated for 48 hrs. The populations followed up were segregated based on their sex ((g) males, (f) females) and separated into groups of 25 flies/vial. Approximately half of the flies were fed with 0.2 mg/ml RU486 to induce dominant negative EcR expression in progenitors and the other half were fed with vehicle. RU486 or vehicle (ethanol) were deposited on the food vials 4–6 hrs before flipping the flies into the vials at 48 hr intervals. Dead flies were visually identified and recorded. Life span assays were performed in two replicates and for each replicate percentage survival was plotted as a function of days elapsed after the start of the assay. Statistical analysis was performed using log rank test. χ^2 represents chi-squared value and the *P* values were provided from pairwise comparison with Bonferroni correction. (i) show experimental details and % mortality of the male or female replicates. Exact *n* numbers and *P* values >0.0001 can be found in the online source data.

Supplementary Material

Refer to Web version on PubMed Central for supplementary material.

ACKNOWLEDGMENTS

We thank Jun Zhou, Irene Miguel-Aliaga, Carl Thummel, Parthive Patel and Lucy O'Brien for stocks and discussions. We thank Omar Salem of McMaster Immunology Research Centre for Fig 3i and Mohamed AbdelMoety of American University of the Middle East for the chemical structure in Fig 3i. This work was supported by ERC AdG 268515, DFG SFB873 and NIH GM124434 to B.A.E., and by the Helmholtz Zukunftsthema "Aging and Metabolic Programming" (AMPro) to A.A.T.

REFERENCES

1. Capel B Vertebrate sex determination: evolutionary plasticity of a fundamental switch. *Nat Rev Genet* 18, 675–689, doi:10.1038/nrg.2017.60 (2017). [PubMed: 28804140]
2. Hudry B, Khadayate S & Miguel-Aliaga I The sexual identity of adult intestinal stem cells controls organ size and plasticity. *Nature* 530, 344–348, doi:10.1038/nature16953 (2016). [PubMed: 26887495]

3. Sieber MH & Spradling AC Steroid Signaling Establishes a Female Metabolic State and Regulates SREBP to Control Oocyte Lipid Accumulation. *Curr Biol* 25, 993–1004, doi:10.1016/j.cub.2015.02.019 (2015). [PubMed: 25802149]
4. Ober C, Loisel DA & Gilad Y Sex-specific genetic architecture of human disease. *Nat Rev Genet* 9, 911–922, doi:10.1038/nrg2415 (2008). [PubMed: 19002143]
5. Schwedes CC & Carney GE Ecdysone signaling in adult *Drosophila melanogaster*. *J Insect Physiol* 58, 293–302, doi:10.1016/j.jinsphys.2012.01.013 (2012). [PubMed: 22310011]
6. Lavrynenko O et al. The ecdysteroidome of *Drosophila*: influence of diet and development. *Development (Cambridge, England)* 142, 3758–3768, doi:10.1242/dev.124982 (2015).
7. Ameku T & Niwa R Mating-Induced Increase in Germline Stem Cells via the Neuroendocrine System in Female *Drosophila*. *PLoS Genet* 12, e1006123, doi:10.1371/journal.pgen.1006123 (2016). [PubMed: 27310920]
8. Meiselman M et al. Endocrine network essential for reproductive success in *Drosophila melanogaster*. *Proc Natl Acad Sci U S A* 114, E3849–E3858, doi:10.1073/pnas.1620760114 (2017). [PubMed: 28439025]
9. Simon AF, Shih C, Mack A & Benzer S Steroid control of longevity in *Drosophila melanogaster*. *Science (New York, N.Y.)* 299, 1407–1410, doi:10.1126/science.1080539 (2003).
10. Tricoire H et al. The steroid hormone receptor EcR finely modulates *Drosophila* lifespan during adulthood in a sex-specific manner. *Mech Ageing Dev* 130, 547–552, doi:10.1016/j.mad.2009.05.004 (2009). [PubMed: 19486910]
11. Jiang H et al. Cytokine/Jak/Stat signaling mediates regeneration and homeostasis in the *Drosophila* midgut. *Cell* 137, 1343–1355, doi:10.1016/j.cell.2009.05.014 (2009). [PubMed: 19563763]
12. Regan JC et al. Sex difference in pathology of the ageing gut mediates the greater response of female lifespan to dietary restriction. *Elife* 5, e10956, doi:10.7554/eLife.10956 (2016). [PubMed: 26878754]
13. Jiang H, Grenley MO, Bravo MJ, Blumhagen RZ & Edgar BA EGFR/Ras/MAPK signaling mediates adult midgut epithelial homeostasis and regeneration in *Drosophila*. *Cell Stem Cell* 8, 84–95, doi:10.1016/j.stem.2010.11.026 (2011). [PubMed: 21167805]
14. Zhang P et al. An SH3PX1-Dependent Endocytosis-Autophagy Network Restrains Intestinal Stem Cell Proliferation by Counteracting EGFR-ERK Signaling. *Dev Cell* 49, 574–589, doi:10.1016/j.devcel.2019.03.029 (2019). [PubMed: 31006650]
15. Reiff T et al. Endocrine remodelling of the adult intestine sustains reproduction in *Drosophila*. *Elife* 4, e06930, doi:10.7554/eLife.06930 (2015). [PubMed: 26216039]
16. Ono H et al. Spook and Spookier code for stage-specific components of the ecdysone biosynthetic pathway in Diptera. *Developmental biology* 298, 555–570, doi:10.1016/j.ydbio.2006.07.023 (2006). [PubMed: 16949568]
17. Marvin KA et al. Nuclear receptors homo sapiens Rev-erb β and *Drosophila melanogaster* E75 are thiolate-ligated heme proteins which undergo redox-mediated ligand switching and bind CO and NO. *Biochemistry* 48, 7056–7071, doi:10.1021/bi900697c (2009). [PubMed: 19405475]
18. White KP, Hurban P, Watanabe T & Hogness DS Coordination of *Drosophila* metamorphosis by two ecdysone-induced nuclear receptors. *Science* 276, 114–117 (1997). [PubMed: 9082981]
19. Biteau B, Hochmuth CE & Jasper H JNK activity in somatic stem cells causes loss of tissue homeostasis in the aging *Drosophila* gut. *Cell Stem Cell* 3, 442–455, doi:10.1016/j.stem.2008.07.024 (2008). [PubMed: 18940735]
20. Biteau B et al. Lifespan extension by preserving proliferative homeostasis in *Drosophila*. *PLoS genetics* 6, e1001159, doi:10.1371/journal.pgen.1001159 (2010). [PubMed: 20976250]
21. Patel PH, Dutta D & Edgar BA Niche appropriation by *Drosophila* intestinal stem cell tumours. *Nat Cell Biol* 17, 1182–1192, doi:10.1038/ncb3214 (2015). [PubMed: 26237646]
22. O'Brien DM, Min K-J, Larsen T & Tatar M Use of stable isotopes to examine how dietary restriction extends *Drosophila* lifespan. *Current Biology* 18, R155–R156, doi:10.1016/j.cub.2008.01.021 (2008). [PubMed: 18302914]
23. Speakman JR The physiological costs of reproduction in small mammals. *Philos Trans R Soc Lond B Biol Sci* 363, 375–398, doi:10.1098/rstb.2007.2145 (2008). [PubMed: 17686735]

24. Hammond KA Adaptation of the maternal intestine during lactation. *J Mammary Gland Biol Neoplasia* 2, 243–252 (1997). [PubMed: 10882308]
25. Amos-Landgraf JM et al. Sex disparity in colonic adenomagenesis involves promotion by male hormones, not protection by female hormones. *Proc Natl Acad Sci U S A* 111, 16514–16519, doi:10.1073/pnas.1323064111 (2014). [PubMed: 25368192]
26. Manson JE et al. Menopausal Hormone Therapy and Long-term All-Cause and Cause-Specific Mortality: The Women’s Health Initiative Randomized Trials. *Jama* 318, 927–938, doi:10.1001/jama.2017.11217 (2017). [PubMed: 28898378]
27. Gunter MJ et al. Insulin, insulin-like growth factor-I, endogenous estradiol, and risk of colorectal cancer in postmenopausal women. *Cancer Res* 68, 329–337, doi:10.1158/0008-5472.Can-07-2946 (2008). [PubMed: 18172327]

EXTENDED REFERENCES

28. Micchelli CA & Perrimon N Evidence that stem cells reside in the adult *Drosophila* midgut epithelium. *Nature* 439, 475–479, doi:10.1038/nature04371 (2006). [PubMed: 16340959]
29. Jiang H & Edgar BA EGFR signaling regulates the proliferation of *Drosophila* adult midgut progenitors. *Development (Cambridge, England)* 136, 483–493, doi:10.1242/dev.026955 (2009).
30. Agaisse H, Petersen U-M, Boutros M, Mathey-Prevot B & Perrimon N Signaling Role of Hemocytes in *Drosophila* JAK/STAT-Dependent Response to Septic Injury. *Developmental Cell* 5, 441–450, doi:10.1016/S1534-5807(03)00244-2 (2003). [PubMed: 12967563]
31. Lee T & Luo L Mosaic analysis with a repressible cell marker for studies of gene function in neuronal morphogenesis. *Neuron* 22, 451–461 (1999). [PubMed: 10197526]
32. Palanker L et al. Dynamic regulation of *Drosophila* nuclear receptor activity in vivo. *Development (Cambridge, England)* 133, 3549–3562, doi:10.1242/dev.02512 (2006).
33. Kozlova T & Thummel CS Spatial patterns of ecdysteroid receptor activation during the onset of *Drosophila* metamorphosis. *Development* 129, 1739–1750 (2002). [PubMed: 11923209]
34. Han SK et al. OASIS 2: online application for survival analysis 2 with features for the analysis of maximal lifespan and healthspan in aging research. *Oncotarget* 7, 56147–56152, doi:10.18632/oncotarget.11269 (2016). [PubMed: 27528229]
35. Schindelin J et al. Fiji: an open-source platform for biological-image analysis. *Nature methods* 9, 676–682, doi:10.1038/nmeth.2019 (2012). [PubMed: 22743772]
36. Liang J, Balachandra S, Ngo S & O’Brien LE Feedback regulation of steady-state epithelial turnover and organ size. *Nature* 548, 588–591, doi:10.1038/nature23678 (2017). [PubMed: 28847000]
37. Zheng W et al. Dehydration triggers ecdysone-mediated recognition-protein priming and elevated anti-bacterial immune responses in *Drosophila* Malpighian tubule renal cells. *BMC biology* 16, 60, doi:10.1186/s12915-018-0532-5 (2018). [PubMed: 29855367]
38. Su Y-H et al. Diet regulates membrane extension and survival of niche escort cells for germline homeostasis via insulin signaling. *Development (Cambridge, England)* 145, dev159186, doi:10.1242/dev.159186 (2018).
39. Caceres L et al. Nitric oxide coordinates metabolism, growth, and development via the nuclear receptor E75. *Genes Dev* 25, 1476–1485, doi:10.1101/gad.2064111 (2011). [PubMed: 21715559]

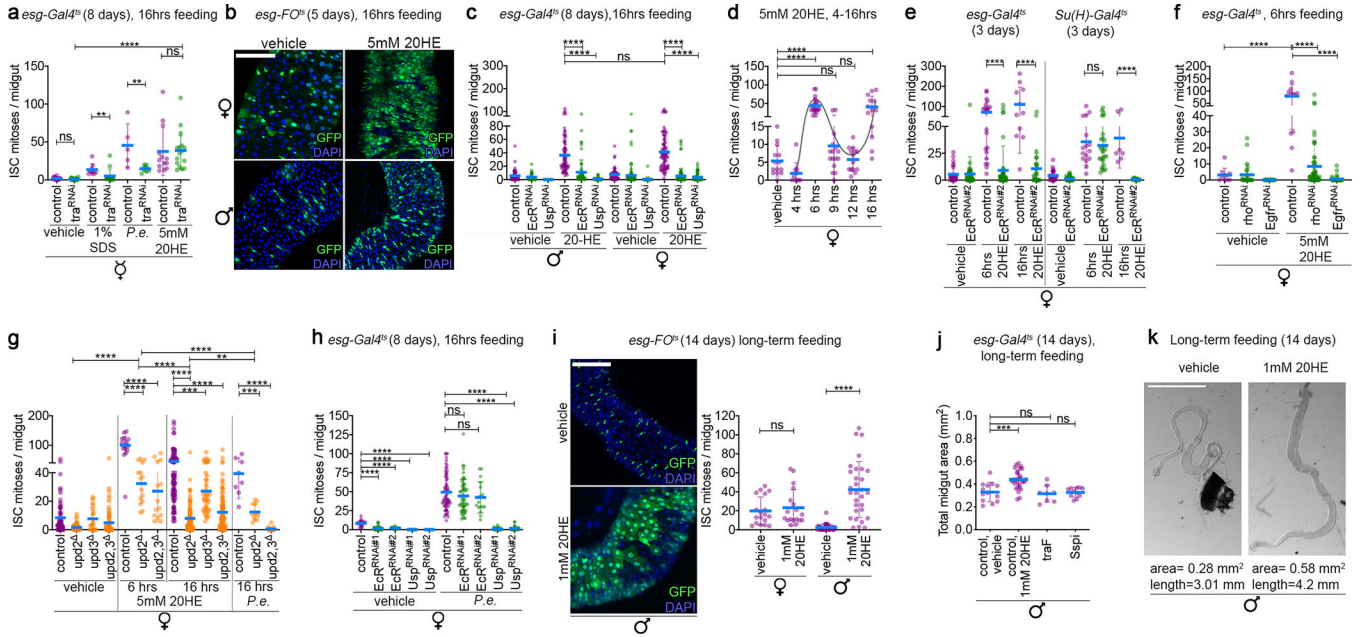


Figure 1: Ecdysone induces ISC proliferation and gut growth.
(a) Midgut mitotic counts of *esgGal4^{ts}>UAS-tra^{RNAi}* virgins after overnight *Pseudomonas entomophila* (*P.e.*) infection, 5mM 20HE or SDS feeding. The *esgGal4^{ts}* driver (*esg-Gal4 tub-Gal80^S*) activates UAS target gene expression specifically in ISC and EBs (“progenitor” cells). **(b)** ISC lineage tracing using *esg-FO^{ts}*, which drives UAS target gene expression in progenitor cells and their newborn progeny (ECs, EBs) following a temperature shift. **(c)** Midgut mitotic counts of *esgGal4^{ts}>EcR^{RNAi}* and *esgGal4^{ts}>Usp^{RNAi}* animals fed 5mM 20HE for 16hrs. **(d)** Midgut mitotic counts from *w¹¹¹⁸* controls fed 5mM 20HE for different durations. **(e)** ISC mitoses in midguts expressing *EcR^{RNAi}* in ISCs+EBs (left) or EBs (right) after 6 or 16hrs of 5mM 20HE feeding. **(f)** Mitotic counts in midguts expressing *rho^{RNAi}* or *Egfr^{RNAi}* in ISCs+EBs 6hrs after 20HE feeding. **(g)** Midgut mitotic counts of *upd2*, *upd3*, *upd2,3* 5–7 day old mutant and control flies after 6 and 16hrs of 5mM 20HE feeding or *P.e.* infection. **(h)** Mitoses of *EcR^{RNAi}* or *Usp^{RNAi}* expressing ISCs+EBs after *P.e.* infection. **(i)** 20HE-fed *esgF/O^{ts}* lineage tracing experiment and mitotic counts. **(j)** Midgut areas from male midguts expressing feminizing TraF or sSpi, or fed with 20HE for 14d. **(k)** Male midgut images. All data shown as mean ± standard deviation; *P* values by Mann–Whitney (1a-i) or ordinary ANOVA test, followed by Bonferroni’s multiple comparisons test. Throughout the manuscript, ns (not significant) is defined as *p* > 0.05; * is defined as *P* 0.05, ** as *P* 0.01**, *** as *P* < 0.001, and **** as *P* < 0.0001. Exact *n* values and *P* values > 0.0001 can be found in the online source data files. *n* 3 independent experiments. GFP: green; DAPI(DNA): blue. Scale bars (b, i) = 100 μm, (k) = 1 mm. ♂: males. ♀: virgin females. ♀: mated females.

virgin and 48h or 72h mated female midguts expressing *EcR^{RNAi}* in EBs using the EB-specific *Su(H)-Gal4^{ts}* driver. **(h)** Midgut mitoses after depletion of 20HE synthetic enzymes by RNAi using the ovary-specific driver *c587-Gal4^{ts}*. **(i)** Midgut areas of whole-body *spo* mutants (*spo^{Z339/Df}*) rescued to adulthood by an exogenous 20HE pulse given to embryos, and controls (*spo^{Z339/+}*). **(j)** Ovary-derived 20HE promotes gut ISC number. **(k)** Images and counts of percent positive delta cells or EBs as a fraction of total cells/region in R4. **(l)** qRT-PCR of *Eip75B* and *broad* mRNA in whole 20HE-fed or mated midguts. **(m)** Mitoses of *Eip75B^{RNAi}* ISC clones \pm heme or 20HE. **(n)** Mitotic counts of ISC clones overexpressing *Eip75B*. **(o)** Epistasis tests assaying interactions between *Eip75B* and *Hr3*. **(p)** Cumulative eggs laid by mated females with progenitor-specific *EcR^{RNAi}* or *Eip75B^{RNAi}*, and controls, \pm s.d. (a-o) Data displayed as mean \pm s.d.; *P* values by ordinary ANOVA test, followed by Bonferroni's multiple comparisons test (2c,e) or Mann-Whitney (others). (ns: *P*>0.05, **P* 0.05, ***P* 0.01, ****P*<0.001, *****P*<0.0001). Representative images are shown, *n* 3 independent experiments. GFP: green; DAPI(DNA): blue. Scale bars (b, e, k) = 100 μ m, (d) = 1 mm. Exact *n* values and *P* values >0.0001 can be found in the online source data files.

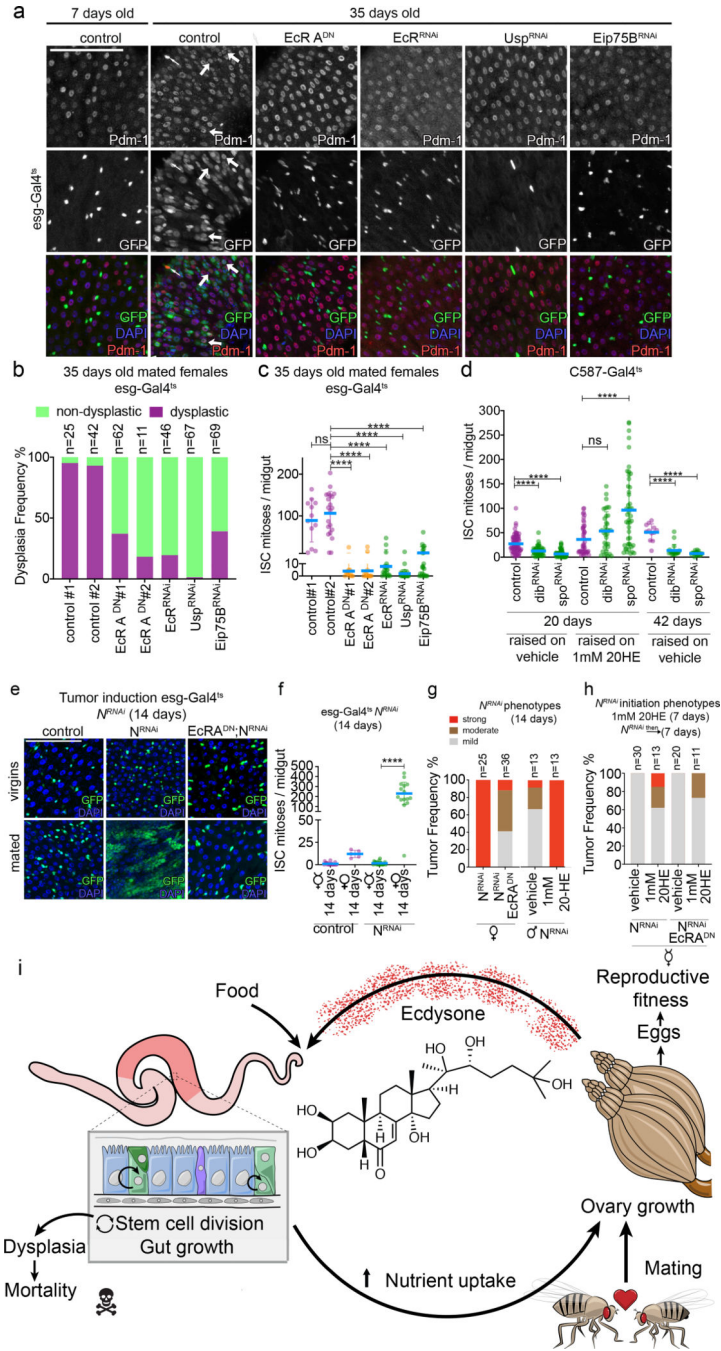


Figure 3: Exogenous and mating-dependent 20HE promote intestinal dysplasia and tumorigenesis.

(a) Aging control females accumulate mis-differentiated cells doubly positive for *esg+* (GFP, green) and EC marker Pdm-1 (red; examples: thick white arrows), that can divide (thin white arrows: PH3+). Intestinal dysplasia is blocked by reduced EcR, Usp, or Eip75B such that progenitors express GFP only. (b) Percentage of midguts classified as dysplastic (purple) or non-dysplastic (green) in region R4. Guts with 10 Pdm1⁺ GFP⁺ progenitors were scored as dysplastic. (c) Mitotic counts of midguts as in (a). (d) Midgut mitoses in females expressing

ovary-targeted RNAi against the ecdysteroidogenic enzymes *dib* or *spo*. **(e)** *Notch^{RNAi}* (*N^{RNAi}*)-expressing ISC tumors (green cells) are induced in mated females by *esg-Gal4^{ts}*, but not in age-matched virgins. Tumor progression is blocked by dominant negative EcR (EcRA DN). **(f)** Mitotic counts as in **(e)**. **(g)** *esg-Gal4^{ts} UAS-N^{RNAi}* tumor type distributions under conditions as classified in ED 10d. **(h)** Tumor distributions of virgin females fed 1mM 20HE for 7d prior to *N^{RNAi}* induction by *esg-Gal4^{ts}*. Representative images are shown, n=3 independent experiments. GFP: green; DAPI(DNA): blue; Pdm-1: red. Scale bars (a,e) = 100 μ m. **(i)** Model summarizing our conclusions. R4 region: red. Data displayed as mean \pm s.d.; *P* values by Mann–Whitney (ns: *P*>0.05, ****: *P*<0.0001). *n* 3 independent experiments. Exact *n* values and *P* values >0.0001 can be found in the online source data files.